

ferases (*FUT1* and *FUT2*) was not recovered by the 5-aza-dC-treatment, implying there might be certain glyco-genes whose expression was not controlled by DNA hypermethylation despite the presence of CpG islands. In the human CRC cell line HCT116 with genetic disruption of both *DNMT1* and *DNMT3b*,¹⁷ in which genomic DNA methylation was nearly eliminated, the expression of *A3GALNT* and *B4GALNT2* was rescued (Figure 2B). Because it has been reported that promoter hypermethylation of the *A3GALNT* gene is associated with the loss of blood group A antigen expression in bladder cancer, oral squamous cell carcinoma, and gastric cancer cell lines,²⁸⁻³⁰ our results suggest that aberrant methylation of the *A3GALNT* gene may lead to a cancer-associated reduction in the level of A antigen in colon cancers. Although remarkable induction of *B4GALNT1* mRNA was observed after 5-aza-dC-treatment, we excluded the *B4GALNT1* gene from subsequent analysis; because the expression of *B4GALNT1* and GM2 gangliosides synthesized by *B4GALNT1* is already known to be increased in GI cancers.³¹ In any case, these results strongly suggest that down-regulation of glycosyltransferases might be the leading cause of cancer-associated abnormal glycosylation and that the *B4GALNT2* gene is a good representative of gene silencing by hypermethylation.

Recovery of Sd^a Carbohydrate Determinant in CRC Cells by Suppression of DNA Methyltransferases

The human *B4GALNT2* gene encodes a β 1,4GalNAcT that is responsible for the synthesis of Sd^a carbohydrate antigen (Sd^a- β 1,4GalNAcT). A noteworthy characteristic of the Sd^a carbohydrate determinant is that its expression is restricted to normal GI mucosa and is strikingly reduced or absent in GI cancer tissue.^{11,12} So we asked if the membrane Sd^a structure could be detected in human CRC cell lines in which DNA methylation was suppressed. Treatment of T84 and HT29 human colonic cancer cell lines, which originally lacked the Sd^a carbohydrate, with 5-aza-dC resulted in an obvious increase in cell-surface expression of Sd^a along with the concomitant induction of *B4GALNT2* expression (Figure 3A and B). When these cells were treated with butyrate, a histone deacetylase inhibitor, neither expression of Sd^a antigen nor *B4GALNT2* mRNA was induced. We found that DNMT1 KO cells strongly expressed Sd^a determinants, whereas the parental HCT116 cells only weakly expressed it (Figure 3C). Furthermore, transcripts of *B4GALNT2* were detected in DNMT1 KO cells, but not in the parental HCT116 cells. These results suggest collectively that DNA hypermethylation rather than histone deacetylation may contribute to the down-regulation of *B4GALNT2* expression in cancer cells.

Methylation Status of B4GALNT2 Gene Promoter Region in GI Cancer Cell Lines and Primary Gastric Carcinomas

Next, we examined the methylation status of the upstream of the *B4GALNT2* gene in gastric cancer cell lines by COBRA. Hypermethylation in the *B4GALNT2* gene was detected in 5 of 6 human gastric cancer cell lines tested (Figure 4A, left). Atypical methylation in the *B4GALNT2* in a primary gastric carcinoma but not in the normal gastric mucosa adjacent to it was also found (Figure 4A, right). Because COBRA reflects the methylation status of only 2 adjoining CpG motifs, PCR products, extending from 169 bp upstream to 217 bp downstream from the translation start site and containing 39 CpGs, were subjected to bisulfite sequencing. Most of the CpGs examined were methylated in gastric cancer cells except in MKN45 cells, which were methylation negative by COBRA (Figure 4B). We also examined the methylation status of the *B4GALNT2* gene in DNMT1/

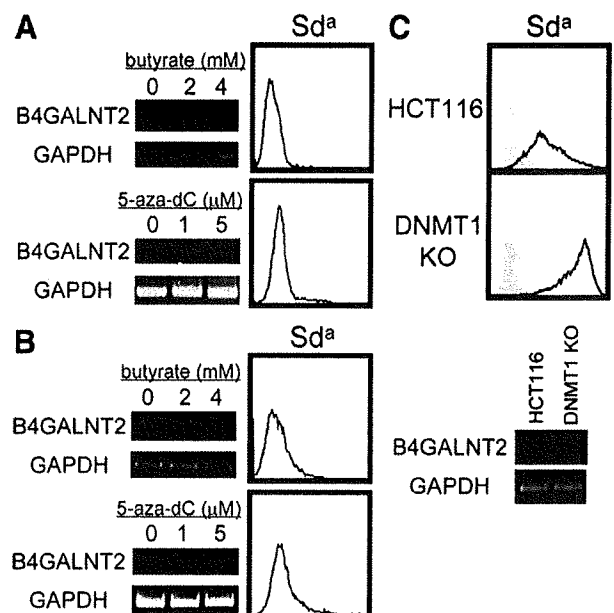


Figure 3. Effects of inhibitors on cell-surface Sd^a antigen and *B4GALNT2* mRNA expression in human CRC cells. Human CRC cell line T84 (A) and HT29 (B) were treated with the histone deacetylase inhibitor butyrate (upper panels) or the methyltransferase inhibitor 5-aza-dC at the concentrations indicated (lower panels). For RT-PCR analysis, cells were collected after 3 days of treatment, and expression levels of *B4GALNT2* and *GAPDH* were then assessed. For flow cytometric analysis, cells were treated with 4 μ mol/L butyrate (upper panels) or 5 μ mol/L 5-aza-dC (lower panels) for 6 days and then were stained with mAb KM694 (specific for Sd^a). Filled histograms represent the control staining of untreated cells. (C) Human CRC cell line HCT116 and DNMT1 KO cells were stained with mAb KM694 and then analyzed by flow cytometry. Filled histograms represent the control staining without mAb (upper panels). HCT 116 and DNMT1 KO cells were also assessed for expression levels of *B4GALNT2* and *GAPDH* by RT-PCR (lower panels). The data are representative of 3 separate experiments, which gave similar results.

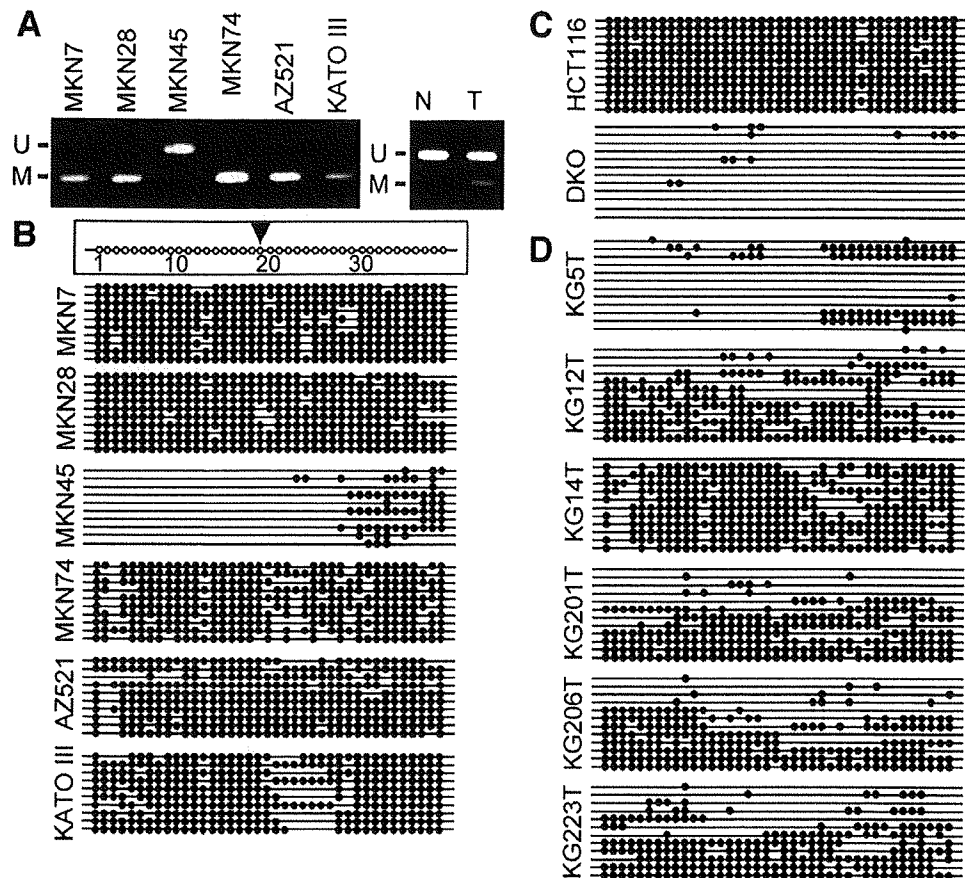


Figure 4. Methylation of the *B4GALNT2* gene in gastric cancer cells and primary gastric carcinomas. (A) Combined bisulfite restriction analysis (COBRA) of human gastric cancer cell lines (left) and representative results for a primary gastric carcinoma (right). M, methylated alleles; N, gastric normal mucosa adjacent to the tumor; T, gastric tumor; U, unmethylated alleles. (B, C and D) Methylation status of individual CpG residues in the *B4GALNT2* gene in human gastric cancer cell lines (B), human CRC cell line HCT116 and DKO cells (C), and primary gastric carcinomas (D) assessed by bisulfite sequencing. Bisulfite-PCR products cloned into the pCR4-TOPO vector were randomly picked up for sequencing. As illustrated in the box at the top of B, the line indicates an independent clone of bisulfite-PCR products; it contains 39 consecutive CpGs (open circles). For sequencing of the bisulfite-PCR product, the DNA fragment was purified and cloned into the pCR4-TOPO vector (Invitrogen). The start site of translation is indicated by the arrowhead. In the results shown below this box, the filled circles on the lines for each clone appear only when CpGs are methylated. Cell lines and case ID of tumors are shown at the left in B and C, respectively.

DNMT3b DKO cells. As expected, methylated CpGs were hardly seen in DKO cells, whereas most of the CpGs examined were methylated in the parental HCT116 cells (Figure 4C). Furthermore, it was clearly evident that the upstream of the *B4GALNT2* gene was frequently hypermethylated in human gastric cancer tissues (Figure 4D). Sample KG5T, methylation negative by COBRA, and MKN45 cells looked less methylated but included apparently hypermethylated clones. These results imply that DNA hypermethylation in the promoter region of the *B4GALNT2* gene may have contributed to the down-regulation of *B4GALNT2* expression in gastric cancers.

Methylation Status of *B4GALNT2* Gene and Clinicopathologic Characteristics in Primary Gastric Carcinomas

To understand the significance of hypermethylation in the *B4GALNT2* gene, we analyzed the methylation status

of the *B4GALNT2* gene and clinicopathologic characteristics of patients with gastric carcinomas. We deemed that the *B4GALNT2* gene was methylated when the percentage of methylated DNA was $\geq 10\%$ by COBRA. Of the 78 primary gastric tumors studied, 39 were classified as methylation positive (Table 1). Univariate analysis revealed no difference between the methylation-positive and -negative groups with respect to age, gender, tumor location, macroscopic type, lymphatic invasion, venous invasion, or pT, pN, or pM status. However, there were significant differences between patients in the methylation-positive and -negative groups with respect to histology ($P = .012$) and EBV status ($P = .001$). EBV was detected in 10 of the 78 tumors, and all EBV-associated tumors were methylation-positive ones. No difference was noted in the frequency of *p53* mutation or the infection of HP between the methylation-positive and -negative groups. To examine the correlation between the

Table 1. Clinicopathologic Features of Gastric Cancer With or Without Methylation of *B4GALNT2*

Characteristics	Total	Number of patients (%)		P-value
		Methylated	Unmethylated	
Number of patients	78	39 (50.0)	39 (50.0)	
Mean age \pm SD (y)		63.6 \pm 13.6	65.4 \pm 10.3	.531
Gender				
Male	52 (66.6)	24 (61.5)	28 (71.8)	.472
Female	26 (33.3)	15 (38.5)	11 (28.2)	
Tumor location				
Upper one third	22 (28.2)	14 (35.9)	8 (20.5)	.279
Middle one third	23 (29.5)	9 (23.1)	14 (35.9)	
Lower one third	33 (42.3)	16 (41.0)	17 (43.6)	
Macroscopic type				
0	4 (5.1)	2 (5.1)	2 (5.1)	.98
1	6 (7.7)	3 (7.7)	3 (7.7)	
2	30 (38.5)	14 (35.9)	16 (41.0)	
3	30 (38.5)	15 (38.5)	15 (38.5)	
4	8 (10.3)	5 (12.8)	3 (7.7)	
Histology (Lauren)				
Intestinal	36 (46.2)	12 (30.8)	24 (61.5)	.012
Diffuse	42 (53.8)	27 (69.2)	15 (38.5)	
Lymphatic invasion				
Negative	20 (25.6)	9 (23.1)	11 (28.2)	.78
Positive	58 (74.4)	30 (76.9)	28 (71.8)	
Venous invasion				
Negative	37 (47.4)	20 (51.3)	17 (43.6)	.651
Positive	41 (52.6)	19 (48.7)	22 (56.4)	
Pathologic tumor classification				
pT1	5 (6.4)	3 (7.7)	2 (5.1)	.407
pT2	43 (55.1)	19 (48.7)	24 (61.5)	
pT3	28 (35.9)	15 (38.5)	13 (33.3)	
pT4	2 (2.6)	2 (5.1)	0 (0.0)	
Pathologic lymph node status				
pN0	22 (28.2)	9 (23.1)	13 (33.3)	.373
pN1	28 (35.9)	15 (38.5)	13 (33.3)	
pN2	16 (20.5)	8 (20.5)	8 (20.5)	
pN3	12 (15.4)	7 (17.9)	5 (12.8)	
Pathologic metastasis status				
pM0	66 (84.6)	36 (92.3)	30 (76.9)	.114
pM1	12 (15.4)	3 (7.7)	9 (23.1)	
Stage (pTNM)				
I	18 (23.1)	8 (20.5)	10 (25.6)	.804
II	16 (20.5)	8 (20.5)	8 (20.5)	
III	21 (26.9)	12 (30.8)	9 (23.1)	
IV	23 (29.5)	11 (28.2)	12 (30.8)	
<i>Helicobacter pylori</i>				
Positive	65 (83.3)	33 (84.6)	32 (82.1)	.999
Negative	13 (16.7)	6 (15.4)	7 (17.9)	
Epstein-Barr virus				
Positive	10 (12.8)	10 (25.6)	0 (0.0)	.001
Negative	68 (87.2)	29 (74.4)	39 (100.0)	
p53 mutation				
Positive	19 (24.4)	6 (15.4)	13 (33.3)	.112
Negative	59 (75.6)	33 (84.6)	26 (66.7)	

SD, standard deviation; pTNM, pathologic tumor, lymph node, metastasis status according to the International Union Against Cancer classification system.

Sd^a expression and DNA hypermethylation of *B4GALNT2*, we determined the expression levels of Sd^a carbohydrates in freshly frozen gastric cancers, because Sd^a antigen is expressed as a glycolipid in the stomach; its reactivity to antibodies was lost in formalin-fixed paraffin-embedded

samples that we used for our clinicopathologic analysis. Of the 15 freshly frozen gastric cancers studied, the expression of Sd^a determinants was totally lost in all cases as determined by immunohistologic staining; 7 cases were methylation positive by COBRA (data not shown).

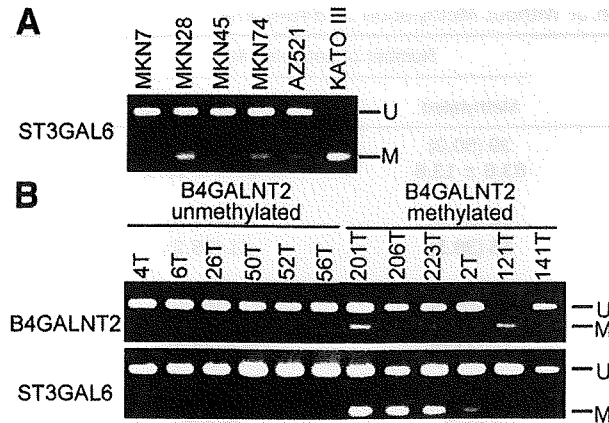


Figure 5. Methylation of *B4GALNT2* and *ST3GAL6* genes in gastric cancer cells and primary gastric carcinomas. Representative results are shown from COBRA using human gastric cancer cell lines (A) and primary tumors (B). M, methylated alleles; U, unmethylated alleles. The genes that were analyzed are shown on the left.

Methylation Status of Glyco-Genes in Gastric Cancer Cell Lines and Primary Gastric Carcinomas

Finally, we examined whether epigenetic changes occurred in the *ST3GAL6* gene together with those in the *B4GALNT2* gene in human gastric cancer cells. Of the cancer-associated down-regulated glyco-genes that we found in the present study, the *ST3GAL6* was hypermethylated in concurrence with methylation of the *B4GALNT2* in many of the gastric cancer cell lines as well as in gastric cancer tissues (Figure 4A and Figure 5). As shown in Table 2, aberrant methylation in the *ST3GAL6* was detected in 24 of 32 primary gastric tumors with statistically significant correlation with the methylation of *B4GALNT2* and EBV status ($P < .01$). No difference was noted in the frequency of *p53* mutation between the *ST3GAL6*-methylated and -unmethylated groups. These results strongly suggest that epigenetic changes may occur in a group of glyco-genes including *B4GALNT2* and *ST3GAL6* in gastric cancer tissues, which may eventually induce aberrant glycosylation and expression of cancer-associated carbohydrate antigens by silencing the enzyme activity responsible for antigen expression.

Discussion

Aberrant glycosylation, which would be expected to eventually induce the expression of cancer-associated carbohydrate antigens, has been observed in many types of tumors. In the aspect of carbohydrate synthesis, here we clearly demonstrated that the down-regulation of a set of glyco-genes involved in carbohydrate biosynthetic pathways is a major event in the cancer, rather than the up-regulation of certain glycosyltransferases. Cancer-specific DNA hypermethylation played a significant role in

this gene silencing. We further extended the analysis to 93 gastric cancer tissues and, for the first time, found a high frequency of DNA hypermethylation in glyco-genes. The significance of these issues is discussed below.

Recent studies including ours suggest clearly that the precise mechanism for up-regulation of cancer-associated carbohydrate antigens revolves not necessarily around the enhancement of glycosylation in tumors, but rather around the down-regulation of glyco-genes that are involved in the synthesis of normally expressed determinants, such as Sd^a, disialyl Lewis^a, and so on.^{15,32-34} In our results, the CpG islands of the *B4GALNT2* gene encoding Sd^a-β1,4GalNAcT, the enzyme responsible for the synthesis of the Sd^a structure, were densely methylated; and this methylation was closely correlated with the transcriptional silencing of the *B4GALNT2* gene. Because DNA hypermethylation of the *B4GALNT2* gene was detected in 50% of our gastric cancer cases examined by COBRA, this hypermethylation seems to be an important molecular mechanism well explaining the down-regulation of Sd^a. Our present study using freshly frozen samples reconfirmed our previous report that nearly 100% of gastric cancers showed loss of Sd^a antigen.¹² We believe that the difference in frequency between DNA hypermethylation and loss of Sd^a may be attributed to the rather dull sensitivity of COBRA. For example, MKN45 cells were methylation negative by COBRA, despite the apparent hypermethylation of certain areas in the promoter region as assessed by bisulfite sequencing (Figure 4A, B). Besides, in the case of the *B4GALNT2* gene and Sd^a antigens, the methylation status of the *A3GALNT* gene, encoding the enzyme responsible for the synthesis of the blood group A and B determinants, correlates well with the expression of the blood group A and B determinants in gastric

Table 2. Methylation Status of *B4GALNT2*, EBV Infection, and *P53* Mutation of Gastric Cancer With or Without Methylation of *ST3GAL6*

Characteristic	Number of patients (%)		
	Total	<i>ST3GAL6</i>	
		Methylated	Unmethylated
Number of patients	63	28 (44.4)	35 (55.6)
<i>B4GALNT2</i> ^a			
Methylated	32 (50.8)	24 (85.7)	8 (22.9)
Unmethylated	31 (49.2)	4 (14.3)	27 (77.1)
Epstein-Barr virus ^a			
Positive	9 (14.3)	8 (28.6)	1 (2.9)
Negative	54 (85.7)	20 (71.4)	34 (97.1)
<i>p53</i> mutation			
Positive	15 (23.8)	6 (21.4)	9 (25.7)
Negative	48 (76.2)	22 (78.6)	26 (74.3)

NOTE. Methylation of *ST3GAL6* was compared by using the Fisher exact test for methylation of *B4GALNT2*, EBV association, and *p53* mutation.

^aStatistically significant ($P < .01$).

cancer cell lines including MKN28, MKN45, and KATO III cells.³⁰ We reported earlier that forced expression of Sd^a-β1,4GalNAcT resulted in a marked increase in cell-surface expression of Sd^a along with a concomitant loss of cancer-associated sLe^{x/a} carbohydrate antigens.¹⁵ Of note, DNA hypermethylation of *B4GALNT2* gene may be associated with the concomitant increase in sLe^{x/a} in GI cancers as a typical example of “incomplete synthesis” for abnormal expression of carbohydrate determinants. In addition, we reaffirmed that DNA methylation contributes to the cancer-associated silencing of the *A3GALNT* gene in GI cancer cells. In bladder cancers and oral squamous cell carcinomas, a relationship between decreased expression of the blood group A and B determinants and allelic loss and/or hypermethylation of the *A3GALNT* gene has been reported.^{28,29,35} DNA hypermethylation of this gene in GI cancers may also lead to enhanced expression of sLe^{x/a} consequent to a reduction in blood group A antigen.

Further, our report provides the first description of a relationship between the methylation status of glycosyltransferase and clinicopathologic features. Throughout the present study, we observed a strong correlation between promoter methylation of the *B4GALNT2* gene and EBV-associated gastric carcinoma (Table 1). The frequency of *B4GALNT2* methylation in EBV-associated tumors was 100%. EBV is a ubiquitous herpes virus that infects most children during early childhood and is involved in a subset of gastric carcinomas, although its specific role in carcinogenesis remains unclear. It has been shown that the expression of tumor-suppressor genes, such as p16 cyclin-dependent kinase 4A inhibitor (p16^{INK4A}), is absent significantly more often in EBV-associated gastric carcinomas than in EBV-negative ones and that their loss is associated with their methylation.³⁶ Our finding is consistent with former reports indicating that carcinogenesis of EBV-associated gastric tumors commonly involves hypermethylation of multiple genes. Extensive studies on the molecular mechanism underlying oncogenic virus-related aberrant methylation have been carried out. It was reported that oncogenic virus-related aberrant methylation was caused by DNMT3b up-regulation via Ras activation.³⁷ It is plausible that aberrant methylation seen in EBV-associated gastric tumors may be based on the same molecular machinery. Furthermore, in the present study, approximately three fourths of the *B4GALNT2* methylation-positive carcinomas were EBV negative; therefore, increased methylation of this gene in tumors without EBV association might be mediated by some different, as yet unknown mechanism. HP infection of the stomach is also a significant factor related to carcinogenesis.³⁸ No correlation was observed between hypermethylation of *B4GALNT2* and HP status, although HP infection is extraordinarily common (83.3% in Table 1). These results suggest collectively that aberrant

methylation of *B4GALNT2* might be induced by factors independent of those related to HP infection.

Another important finding of this study was that the hypermethylation occurred coincidentally in *B4GALNT2* and *ST3GAL6* genes, as was clearly shown in Figure 5 and Table 2. Because the human *ST3GAL6* gene encodes the α2,3-sialyltransferase responsible for the synthesis of type II precursor, the suppression of this gene seems to result in a lesser amount of the precursor for the biosynthesis of the Sd^a determinant. These observations allow us to suppose that epigenetic suppression of multiple glyco-genes, including glycosyltransferases, glycosidases, and mucins in tumors, may not occur in a random manner but in a certain set of them and other genes. We can add on yet the fact that some glyco-genes, whose expression is decreased in cancers and whose promoter regions contain CpG islands, seemed to be controlled epigenetically. Taken together, our data suggest that there might be a certain group of glyco-genes whose expression in cancers is controlled together by DNA hypermethylation. Although more studies on individual glyco-genes are required to support this hypothesis, simultaneous silencing of glycosyltransferases might eventually result in the induction of aberrant glycosylation and expression of cancer-associated carbohydrate antigens by inactivating their enzyme activity. In conclusion, we propose that an epigenetic change such as DNA hypermethylation is one of the major mechanisms causing cancer-associated changes in carbohydrate determinants by silencing normal glycosylation, especially being a part of the mechanism referred to previously as incomplete synthesis.

Supplementary Data

Note: To access the supplementary material accompanying this article, visit the online version of *Gastroenterology* at www.gastrojournal.org, and at doi: 10.1053/j.gastro.2008.03.031.

References

1. Hakomori S. Glycosylation defining cancer malignancy: New wine in an old bottle. *Proc Natl Acad Sci U S A* 2002;99:10231–10233.
2. Nakamori S, Kameyama M, Imaoka S, et al. Increased expression of sialyl Lewisx antigen correlates with poor survival in patients with colorectal carcinoma: clinicopathological and immunohistochemical study. *Cancer Res* 1993;53:3632–3637.
3. Nakayama T, Watanabe M, Katsumata T, et al. Expression of sialyl Lewis^x as a new prognostic factor for patients with advanced colorectal carcinoma. *Cancer* 1995;75:2051–2056.
4. Futamura N, Nakamura S, Tatematsu M, et al. Clinicopathologic significance of sialyl Lex expression in advanced gastric carcinoma. *Br J Cancer* 2000;83:1681–1687.
5. Walz G, Aruffo A, Kolanus W, et al. Recognition by ELAM-1 of the sialyl-Lex determinant on myeloid and tumor cells. *Science* 1990;250:1132–1135.
6. Takada A, Ohmori K, Yoneda T, et al. Contribution of carbohydrate antigens sialyl Lewis A and sialyl Lewis X to adhesion of human cancer cells to vascular endothelium. *Cancer Res* 1993;53:354–361.

7. Ito H, Hiraiwa N, Sawada-Kasugai M, et al. Altered mRNA expression of specific molecular species of fucosyl- and sialyl-transferases in human colorectal cancer tissues. *Int J Cancer* 1997; 71:556–564.
8. Salvini R, Bardoni A, Valli M, et al. β 1,3-Galactosyltransferase β 3Gal-T5 acts on the GlcNAc β 1 \rightarrow 3Gal β 1 \rightarrow 4GlcNAc β 1 \rightarrow R sugar chains of carcinoembryonic antigen and other N-linked glycoproteins and is down-regulated in colon adenocarcinomas. *J Biol Chem* 2001;276:3564–3573.
9. Kumamoto K, Goto Y, Sekikawa K, et al. Increased expression of UDP-galactose transporter messenger RNA in human colon cancer tissues and its implication in synthesis of Thomsen-Friedenreich antigen and sialyl Lewis X/A determinants. *Cancer Res* 2001;61:4620–4627.
10. Hakomori S. Tumor-associated glycolipid antigens defined by monoclonal antibodies. *Bull Cancer* 1983;70:118–126.
11. Morton JA, Pickles MM, Terry AM. The Sda blood group antigen in tissues and body fluids. *Immunol Invest* 1988;17:217–224.
12. Dohi T, Ohta S, Hanai N, et al. Sialypentaosylceramide detected with anti-GM2 monoclonal antibody. Structural characterization and complementary expression with GM2 in gastric cancer and normal gastric mucosa. *J Biol Chem* 1990;265:7880–7885.
13. Dohi T, Nishikawa A, Ishizuka I, et al. Substrate specificity and distribution of UDP-GalNAc:sialylparagloboside N-acetylgalactosaminyltransferase in the human stomach. *Biochem J* 1992; 288:161–165.
14. Dohi T, Hanai N, Yamaguchi K, et al. Localization of UDP-GalNAc: NeuAc α 2,3Gal-R β 1,4(GalNAc to Gal)N-acetylgalactosaminyltransferase in human stomach. Enzymatic synthesis of a fundic gland-specific ganglioside and GM2. *J Biol Chem* 1991;266: 24038–24043.
15. Kawamura YI, Kawashima R, Fukunaga R, et al. Introduction of Sda carbohydrate antigen in gastrointestinal cancer cells eliminates selectin ligands and inhibits metastasis. *Cancer Res* 2005;65:6220–6227.
16. Jones PA, Baylin SB. The fundamental role of epigenetic events in cancer. *Nat Rev Genet* 2002;3:415–428.
17. Rhee I, Bachman KE, Park BH, et al. DNMT1 and DNMT3b cooperate to silence genes in human cancer cells. *Nature* 2002; 416:552–556.
18. Toyota M, Ho C, Ahuja N, et al. Identification of differentially methylated sequences in colorectal cancer by methylated CpG island amplification. *Cancer Res* 1999;59:2307–2312.
19. Suzuki H, Itoh F, Toyota M, et al. Inactivation of the 14-3-3 sigma gene is associated with 5' CpG island hypermethylation in human cancers. *Cancer Res* 2000;60:4353–4357.
20. Xiong Z, Laird PW. COBRA: a sensitive and quantitative DNA methylation assay. *Nucleic Acids Res* 1997;25:2532–2534.
21. Okajima T, Fukumoto S, Miyazaki H, et al. Molecular cloning of a novel α 2,3-sialyltransferase (ST3Gal VI) that sialylates type II lactosamine structures on glycoproteins and glycolipids. *J Biol Chem* 1999;274:11479–11486.
22. Lo YM, Chan LY, Lo KM, et al. Quantitative analysis of cell-free Epstein-Barr virus DNA in plasma of patients with nasopharyngeal carcinoma. *Cancer Res* 1999;59:1188–1191.
23. Clayton CL, Kleanthous H, Coates PJ, et al. Sensitive detection of *Helicobacter pylori* by using polymerase chain reaction. *J Clin Microbiol* 1992;30:192–200.
24. Rhei E, Bogomolny F, Federici MG, et al. Molecular genetic characterization of BRCA1- and BRCA2-linked hereditary ovarian cancers. *Cancer Res* 1998;58:3193–3196.
25. Japanese Gastric Cancer Association. *Gastric Cancer* 1998;1: 10–24.
26. Sobin LH, Wittekind C, eds. TNM classification of malignant tumors. 5th ed. New York: John Wiley & Sons; 1997.
27. Lauren P. The two histological main types of gastric carcinoma: diffuse and so-called intestinal-type carcinoma. An attempt at a histo-clinical classification. *Acta Pathol Microbiol Scand* 1965; 64:31–49.
28. Chihara Y, Sugano K, Kobayashi A, et al. Loss of blood group A antigen expression in bladder cancer caused by allelic loss and/or methylation of the ABO gene. *Lab Invest* 2005;85:895–907.
29. Gao S, Worm J, Guldborg P, et al. Genetic and epigenetic alterations of the blood group ABO gene in oral squamous cell carcinoma. *Int J Cancer* 2004;109:230–237.
30. Kominato Y, Hata Y, Takizawa H, et al. Expression of human histo-blood group ABO genes is dependent upon DNA methylation of the promoter region. *J Biol Chem* 1999;274:37240–37250.
31. Yuyama Y, Dohi T, Morita H, et al. Enhanced expression of GM2/GD2 synthase mRNA in human gastrointestinal cancer. *Cancer* 1995;75:1273–1280.
32. Miyazaki K, Ohmori K, Izawa M, et al. Loss of disialyl Lewis^x, the ligand for lymphocyte inhibitory receptor sialic acid-binding immunoglobulin-like lectin-7 (Siglec-7) associated with increased sialyl Lewis^x expression on human colon cancers. *Cancer Res* 2004; 64:4498–4505.
33. Yago K, Zenita K, Ginya H, et al. Expression of α -(1,3)-fucosyltransferases which synthesize sialyl Lex and sialyl Lea, the carbohydrate ligands for E- and P-selectins, in human malignant cell lines. *Cancer Res* 1993;53:5559–5565.
34. Majuri M-L, Niemelä R, Tiisala S, et al. Expression and function of α 2,3-sialyl- and α 1,3/1,4-fucosyltransferases in colon adenocarcinoma cell lines: role in synthesis of E-selectin counter-receptors. *Int J Cancer* 1995;63:551–559.
35. Iwamoto S, Withers DA, Handa K, et al. Deletion of A-antigen in a human cancer cell line is associated with reduced promoter activity of CBF/NF-Y binding region, and possibly with enhanced DNA methylation of A transferase promoter. *Glycoconj J* 1999; 16:659–666.
36. Kang GH, Lee S, Kim WH, et al. Epstein-Barr virus-positive gastric carcinoma demonstrates frequent aberrant methylation of multiple genes and constitutes CpG island methylator phenotype-positive gastric carcinoma. *Am J Pathol* 2002;160:787–794.
37. Soejima K, Fang W, Rollins BJ. DNA methyltransferase 3b contributes to oncogenic transformation induced by SV40T antigen and activated Ras. *Oncogene* 2003;22:4723–4733.
38. Uemura N, Okamoto S, Yamamoto S, et al. *Helicobacter pylori* infection and the development of gastric cancer. *N Engl J Med* 2001;345:784–789.

Received November 15, 2007. Accepted March 13, 2008.

Address requests for reprints to: Dr Taeko Dohi, Department of Gastroenterology, Research Institute, International Medical Center of Japan, 1-21-1 Toyama, Shinjuku-ku, Tokyo 162-8655, Japan. e-mail: dohi@ri.imcj.go.jp; fax: 81-3-3202-7364.

Supported by grants and contracts from the International Health Cooperation Research; the Ministry of Health, Labor, and Welfare; the program Grants-in-Aid for Scientific Research on Priority Areas and Grants-in-Aid for Young Scientists from the Ministry of Education, Culture, Sports, Science, and Technology; and the Japan Health Sciences Foundation and Organization.

The authors thank Drs Nobuo Hanai, Kenya Shitara, and So Ohta for providing us with monoclonal antibodies, and Ms Miyuki Nakasuji for her technical assistance.

Supplementary Table 1. Human glyco-genes.

Genes	Accession No.	ID of TaqMan probe kits	Enzyme	References
<i>FUT1</i>	NM000148	Hs00355741_m1	α 1,2-fucosyltransferase, H blood group	1, 2
<i>FUT2</i>	NM000511	Hs00704693_s1	α 1,2-fucosyltransferase, Se blood group	3
<i>FUT3</i>	NM000149	Hs00356857_m1	α 1,3/4-fucosyltransferase, Lewis blood group	4
<i>FUT4</i>	NM002033	Hs00275643_s1	α 1,3-fucosyltransferase	5, 6
<i>FUT5</i>	NM002034	Hs00704908_s1	α 1,3-fucosyltransferase	7
<i>FUT6</i>	NM000150	Hs00173404_m1	α 1,3-fucosyltransferase	8
<i>FUT7</i>	NM004479	Hs00237083_m1	α 1,3-fucosyltransferase	9, 10
<i>FUT8</i>	NM178154	Hs00189535_m1	α 1,6-fucosyltransferase	11
<i>A3GALT/A3GALNT</i>	NM020469	Hs00220850_m1	α 1,3- <i>N</i> -galactosyltransferase, α 1,3- <i>N</i> -acetylgalactosaminyltransferase	12, 13
<i>GBGT1</i>	NM021996	Hs00222752_m1	globoside α 1,3- <i>N</i> -acetylgalactosaminyltransferase, Forssman synthetase	14
<i>B3GALNT1</i>	NM003781	Hs00364202_s1	β 1,3- <i>N</i> -acetylgalactosaminyltransferase 1, globoside synthase	15
<i>B3GALNT2</i>	NM152490	Hs00380823_m1	β 1,3- <i>N</i> -acetylgalactosaminyltransferase 2	16
<i>B4GALNT1</i>	NM001478	Hs00155195_m1	β 1,4- <i>N</i> -acetylgalactosaminyltransferase 1, GM2/GD2 synthase	17
<i>B4GALNT2</i>	NM153446	Hs00396440_m1	β 1,4- <i>N</i> -acetylgalactosaminyltransferase 2 Sd ^a synthase	18
<i>B4GALNT3</i>	NM173593	Hs00403843_m1	β 1,4- <i>N</i> -acetylgalactosaminyltransferase 3	19
<i>B4GALNT4</i>	NM178537	Hs00331790_m1	β 1,4- <i>N</i> -acetylgalactosaminyltransferase 4	20
<i>GCNT1</i>	NM001490	Hs00155243_m1	glucosaminyl (<i>N</i> -acetyl) transferase 1, core 2 (β 1,6- <i>N</i> -acetylglucosaminyltransferase)	21
<i>GCNT3</i>	NM004751	Hs00191070_m1	glucosaminyl (<i>N</i> -acetyl) transferase 3	22
<i>GCNT4</i>	NM016591	Hs00275464_s1	glucosaminyl (<i>N</i> -acetyl) transferase 4, core 2 (β 1,6- <i>N</i> -acetylglucosaminyltransferase)	23
<i>ST3GAL1</i>	NM003033	Hs00161688_m1	CMP-NeuAc: β -galactoside α 2,3-sialyltransferase 1	24
<i>ST3GAL2</i>	NM006927	Hs00199480_m1	CMP-NeuAc: β -galactoside α 2,3-sialyltransferase 2	25
<i>ST3GAL3</i>	NM006279	Hs00196718_m1	CMP-NeuAc:Gal β 1,3/4GlcNAc α 2,3-sialyltransferase	26
<i>ST3GAL4</i>	NM006278	Hs00272170_m1	Gal β 1,3/4GlcNAc α 2,3-sialyltransferase	27
<i>ST3GAL5</i>	NM003896	Hs00187405_m1	CMP-NeuAc:lactosylceramide α 2,3-sialyltransferase	28
<i>ST3GAL6</i>	NM006100	Hs00196086_m1	CMP-NeuAc: α 2,3-sialyltransferase	29
<i>ST6GAL1</i>	NM003032	Hs00949382_m1	CMP-NeuAc:galactoside α 2,6-sialyltransferase	30
<i>ST6GAL2</i>	NM032528	Hs00293264_m1	CMP-NeuAc:galactoside α 2,6-sialyltransferase	31
<i>ST6GALNAC1</i>	NM018414	Hs00300842_m1	GalNAc α 2,6-sialyltransferase 1	32
<i>ST6GALNAC2</i>	NM006456	Hs00197670_m1	GalNAc α 2,6-sialyltransferase 2	33
<i>ST6GALNAC3</i>	NM152996	Hs00541761_m1	GalNAc α 2,6-sialyltransferase 3	34
<i>ST6GALNAC4</i>	NM014403	Hs00205241_m1	GalNAc α 2,6-sialyltransferase 4	35
<i>ST6GALNAC5</i>	NM030965	Hs00229612_m1	GalNAc α 2,6-sialyltransferase 5	36
<i>ST6GALNAC6</i>	NM013443	Hs00203739_m1	GalNAc α 2,6-sialyltransferase 6	37
<i>GALNAC4S-6ST</i>	NM015892	Hs00248144_m1	<i>N</i> -acetylgalactosamine 4-sulfate 6- <i>O</i> -sulfotransferase	38
<i>CHST1</i>	NM003654	Hs00186341_m1	galactose-6- <i>O</i> -sulfotransferase	39
<i>CHST2</i>	NM004267	Hs00358839_g1	carbohydrate <i>N</i> -acetylglucosamine-6- <i>O</i> -sulfotransferase 2	40
<i>CHST3</i>	NM004273	Hs00427946_m1	chondroitin 6-sulfotransferase	41
<i>CHST4</i>	NM005769	Hs00428480_m1	<i>N</i> -acetylglucosamine-6- <i>O</i> -sulfotransferase 2, HEC-specific <i>N</i> -acetylglucosamine-6- <i>O</i> -sulfotransferase	42
<i>CHST5</i>	NM012126	Hs00201677_m1	<i>N</i> -acetylglucosamine-6- <i>O</i> -sulfotransferase 3, intestinal <i>N</i> -acetylglucosamine-6- <i>O</i> -sulfotransferase	43
<i>NEU1</i>	NM000434	Hs00166421_m1	sialidase 1, lysosomal sialidase	44
<i>NEU2</i>	NM005383	Hs00193573_m1	sialidase 2, cytosolic sialidase	45
<i>NEU3</i>	NM006656	Hs00198406_m1	sialidase 3, plasma membrane-associated sialidase	46
<i>NEU4</i>	NM080741	Hs00293852_m1	sialidase 4, glyceraldehyde-3-phosphate dehydrogenase	47
<i>GAPDH</i>	NM002046	Hs00266705_g1		

Supplementary References

- Larsen RD, Ernst LK, Nair RP, et al. Molecular cloning, sequence, and expression of a human GDP-L-fucose: β -D-galactoside 2- α -L-fucosyltransferase cDNA that can form the H blood group antigen. *Proc Natl Acad Sci USA* 1990;87:6674–6678.
- Kelly RJ, Ernst LK, Larsen RD, et al. Molecular basis for H blood group deficiency in Bombay (O_h) and para-Bombay individuals. *Proc Natl Acad Sci USA* 1994;91:5843–5847.
- Kelly RJ, Rouquier S, Giorgi D, et al. Sequence and expression of a candidate for the human *secretor* blood group $\alpha(1,2)$ fucosyltransferase gene (FUT2). *J Biol Chem* 1995;270:4640–4649.
- Kukowska-Latallo J, Larsen RD, Nair RP, et al. A cloned human cDNA determines expression of a mouse stage-specific embryonic antigen and the Lewis blood group $\alpha(1,3/1,4)$ fucosyltransferase. *Genes Dev* 1990;4:1288–1303.
- Lowe JB, Stoolman LM, Nair RP, et al. ELAM-1-dependent cell adhesion to vascular endothelium determined by a transfected human fucosyltransferase cDNA. *Cell* 1990;63:475–484.
- Goelz SE, Hession C, Goff D, et al. ELFT: a gene that directs the expression of an ELAM-1 ligand. *Cell* 1990;63:1349–1356.
- Weston BW, Nair RP, Larsen RD, et al. Isolation of a novel human $\alpha(1,3)$ fucosyltransferase gene and molecular comparison to the human Lewis blood group $\alpha(1,3/1,4)$ fucosyltransferase gene. *J Biol Chem* 1992;267:4152–4160.
- Weston BW, Smith PL, Kelly RJ, et al. Molecular cloning of a fourth member of a human $\alpha(1,3)$ fucosyltransferase gene family. *J Biol Chem* 1992;267:24575–24584.
- Sasaki K, Kurata K, Funayama K, et al. Expression cloning of a novel $\alpha(1,3)$ fucosyltransferase that is involved in biosynthesis of the sialyl Lewis x carbohydrate determinants in leukocytes. *J Biol Chem* 1994;269:14730–14737.
- Natsuka S, Gersten KM, Zenita K, et al. Molecular cloning of a cDNA encoding a novel human leukocyte $\alpha(1,3)$ fucosyltransferase capable of synthesizing the sialyl Lewis x determinants. *J Biol Chem* 1994;269:16789–16794.
- Yanagidani S, Uozumi N, Ihara Y, et al. Purification and cDNA cloning of GDP-L-Fuc:*N*-acetyl- β -D-glucosaminide: $\alpha(1-6)$ fucosyltransferase ($\alpha(1-6)$ FucT) from human gastric cancer MKN45 cells. *J Biochem* 1997;121:626–632.
- Yamamoto F, Marken J, Tsuji T, et al. Cloning and characterization of DNA complementary to human UDP-GalNAc: Fuc $\alpha(1\rightarrow2)$ Gal $\alpha(1\rightarrow3)$ GalNAc transferase (histo-blood group A transferase) mRNA. *J Biol Chem* 1990;265:1146–1151.
- Yamamoto F, Clausen H, White T, et al. Molecular genetic basis of the histo-blood group ABO system. *Nature* 1990;345:229–233.
- Xu H, Storch T, Yu M, et al. Characterization of the human Forssman synthetase gene. *J Biol Chem* 1999;274:29390–29398.
- Okajima T, Nakamura Y, Uchikawa M, et al. Expression cloning of human globoside synthase cDNAs. *J Biol Chem* 2000;275:40498–40503.
- Hiruma T, Togayachi A, Okamura K, et al. A novel human $\beta(1,3)$ -*N*-acetylgalactosaminyltransferase that synthesizes a unique carbohydrate structure, GalNAc $\beta(1-3)$ GlcNAc. *J Biol Chem* 2004;279:14087–14095.
- Nagata Y, Yamashiro S, Yodoi J, et al. Expression cloning of $\beta(1,4)$ *N*-acetyltransferase cDNAs that determine the expression of G_{M2} and G_{D2} gangliosides. *J Biol Chem* 1992;267:12082–12089.
- Montiel MD, Krzewinski-Recchi MA, Delannoy P, et al. Molecular cloning, gene organization and expression of the human UDP-GalNAc:Neu5Ac $\alpha(2-3)$ Gal β -R $\beta(1,4)$ -*N*-acetylgalactosaminyltransferase responsible for the biosynthesis of the blood group Sd^a/Cas antigen: evidence for an unusual extended cytoplasmic domain. *Biochem J* 2003;373:369–379.
- Sato T, Gotoh M, Kiyohara K, et al. Molecular cloning and characterization of a novel human $\beta(1,4)$ -*N*-acetylgalactosaminyltransferase, $\beta(4)$ GalNAc-T3, responsible for the synthesis of *N,N'*-diacetyllactosediimine, GalNAc $\beta(1-4)$ GlcNAc. *J Biol Chem* 2003;278:47534–47544.
- Gotoh M, Sato T, Kiyohara K, et al. Molecular cloning and characterization of $\beta(1,4)$ -*N*-acetylgalactosaminyltransferases IV synthesizing *N,N'*-diacetyllactosamine. *FEBS Lett* 2004;562:134–140.
- Bierhuizen MFA, Fukuda M. Expression cloning of a cDNA encoding UDP-GlcNAc:Gal $\beta(1-3)$ GalNAc-R (GlcNAc to GalNAc) $\beta(1-6)$ GlcNAc transferase by gene transfer into CHO cells expressing polyoma large tumor antigen. *Proc Natl Acad Sci USA* 1992;89:9326–9330.
- Yeh JC, Ong E, Fukuda M. Molecular cloning and expression of novel $\beta(1-6)$ -*N*-acetylglucosaminyltransferase that forms core 2, core 4, and I branches. *J Biol Chem* 1999;274:3215–3221.
- Schwientek T, Yeh JC, Levery SB, et al. Control of O-glycan branch formation. Molecular cloning and characterization of a novel thymus-associated core 2 $\beta(1-6)$ -*N*-acetylglucosaminyltransferase. *J Biol Chem* 2000;275:11106–11113.
- Kitagawa H, Paulson JC. Differential expression of five sialyltransferase genes in human tissues. *J Biol Chem* 1994;269:17872–17878.
- Kim YJ, Kin KS, Kim SH, et al. Molecular cloning and expression of human Gal $\beta(1,3)$ GalNAc $\alpha(2,3)$ -sialyltransferase (hST3Gal II). *Biochem Biophys Res Commun* 1996;228:324–327.
- Kitagawa H, Paulson JC. Cloning and expression of human Gal $\beta(1,3)$ (4)GlcNAc $\alpha(2,3)$ -sialyltransferase. *Biochem Biophys Res Commun* 1993;194:375–382.
- Sasaki K, Watanabe E, Kawashima K, et al. Expression cloning of a novel Gal $\beta(1-3/1-4)$ GlcNAc $\alpha(2,3)$ -sialyltransferase using lectin resistance selection. *J Biol Chem* 1993;268:22782–22787.
- Ishii A, Ohta M, Watanabe Y, et al. Expression cloning and functional characterization of human cDNA for ganglioside G_{M3} synthase. *J Biol Chem* 1998;273:31652–31655.
- Okajima T, Fukumoto S, Miyazaki H, et al. Molecular cloning of a novel $\alpha(2,3)$ -sialyltransferase (ST3Gal VI) that sialylates type II lactosamine structures on glycoproteins and glycolipids. *J Biol Chem* 1999;274:11479–11486.
- Grundmann U, Nerlich C, Rein T, et al. Complete cDNA sequence encoding human β -galactoside $\alpha(2,6)$ -sialyltransferase. *Nucleic Acids Res* 1990;18:667.
- Takashima S, Tsuji S, Tsujimoto M. Characterization of the second type of human β -galactoside $\alpha(2,6)$ -sialyltransferase (ST6Gal II), which sialylates Gal $\beta(1,4)$ GlcNAc structures on oligosaccharides preferentially. *J Biol Chem* 2002;277:45719–45728.
- Ikehara Y, Kojima N, Kurosawa N, et al. Cloning and expression of a human gene encoding an *N*-acetylgalactosamine- $\alpha(2,6)$ -sialyltransferase (ST6GalNAc I): a candidate for synthesis of cancer-associated sialyl-Tn antigens. *Glycobiology* 1999;9:1213–1224.
- Samyn-Petit B, Krzewinski-Recchi MA, Steelant WF, et al. Molecular cloning and functional expression of human ST6GalNAc II. Molecular expression in various human cultured cells. *Biochim Biophys Acta* 2000;1474:201–211.
- Tsuchida A, Ogiso M, Nakamura Y, et al. Molecular cloning and expression of human ST6GalNAc III: restricted tissue distribution and substrate specificity. *J Biochem* 2005;138:237–243.
- Harduin-Lepers A, Stokes DC, Steelant WFA, et al. Cloning, expression and gene organization of a human Neu5Ac $\alpha(2-3)$ Gal $\beta(1-3)$ GalNAc $\alpha(2,6)$ -sialyltransferase: hST6GalNAc IV. *Biochem J* 2000;352:37–48.
- Okajima T, Fukumoto S, Ito H, et al. Molecular cloning of brain-specific GD1 α synthase (ST6GalNAc V) containing CAG/glutamine repeats. *J Biol Chem* 1999;274:30557–30562.
- Okajima T, Chen HH, Ito H, et al. Molecular cloning and expression of mouse GD1 α /GD1 α /GQ1b α synthase (ST6GalNAc VI) gene. *J Biol Chem* 2000;275:6717–6723.

38. Ohtake S, Ito Y, Fukuta M, et al. Human N-acetylgalactosamine 4-sulfate 6-O-sulfotransferase cDNA is related to human B cell recombination activating gene-associated gene. *J Biol Chem* 2001;276:43894–43900.
39. Fukuta M, Inazawa J, Torii T, et al. Molecular cloning and characterization of human keratan sulfate Gal-6-sulfotransferase. *J Biol Chem* 1997;272:32321–32328.
40. Li X, Tedder TF. CHST1 and CHST2 sulfotransferases expressed by human vascular endothelial cells: cDNA cloning, expression, and chromosomal localization. *Genomics* 1999;55:345–347.
41. Fukuta M, Kobayashi Y, Uchimura K, et al. Molecular cloning and expression of human chondroitin 6-sulfotransferase. *Biochim Biophys Acta* 1998;1399:57–61.
42. Bistrup A, Bhakta S, Lee JK, et al. Sulfotransferases of two specificities function in the reconstitution of high endothelial cell ligands for L-selectin. *J Cell Biol* 1999;145:899–910.
43. Lee JK, Bhakta S, Rosen SD, et al. Cloning and characterization of a mammalian N-acetylglucosamine-6-transferase that is highly restricted to intestinal tissue. *Biochem Biophys Res Commun* 1999;263:543–549.
44. Bonten E, van der Spoel A, Fornerod M, et al. Characterization of human lysosomal neuraminidase defines the molecular basis of the metabolic storage disorder sialidosis. *Genes Dev* 1996;10:3156–3169.
45. Monti E, Preti A, Rossi E, et al. Cloning and characterization of NEU2, a human gene homologous to rodent soluble sialidases. *Genomics* 1999;57:137–143.
46. Wada T, Yoshikawa Y, Tokuyama S, et al. Cloning, expression, and chromosomal mapping of a human ganglioside sialidase. *Biochem Biophys Res Commun* 1999;261:21–27.
47. Monti E, Bassi MT, Bresciani R, et al. Molecular cloning and characterization of NEU4, the fourth member of the human sialidase gene family. *Genomics* 2004;83:445–453.

Glutamine Increases Autophagy Under Basal and Stressed Conditions in Intestinal Epithelial Cells

TOSHIO SAKIYAMA,* MARK W. MUSCH,* MARK J. ROPELESKI,[†] HIROHITO TSUBOUCHI,[§] and EUGENE B. CHANG*

*Martin Boyer Laboratories, University of Chicago IBD Research Center, Chicago, Illinois; [†]Gastrointestinal Diseases Research Unit, Department of Medicine, Queen's University, Kingston, Ontario, Canada; and the [§]Department of Digestive and Life-Style Related Diseases, Kagoshima University Graduate School of Medical and Dental Sciences, Kagoshima, Japan

Background & Aims: Glutamine plays a protective role in intestinal cells during physiologic stress; however, the protection mechanisms are not fully understood. Autophagy functions in bulk degradation of cellular components, but has been recognized recently as an important mechanism for cell survival under conditions of stress. We therefore sought to see if glutamine's actions involve the induction of autophagy in intestinal cells and, if so, the mechanisms that underlie this action. **Methods:** Formation of microtubule-associated protein light chain 3 (LC3)-phospholipid conjugates (LC3-II) in rat intestinal epithelial IEC-18 cells and human colonic epithelial Caco-2_{BBE} cells was determined by Western blotting and localized by confocal microscopy. Activation of mammalian target of rapamycin (mTOR) pathway, mitogen-activated protein (MAP) kinases, caspase-3, and poly (ADP-ribose) polymerase were monitored by Western blotting. **Results:** Glutamine increased LC3-II as well as the number of autophagosomes. Glutamine-induced LC3-II formation was paralleled by inactivation of mTOR and p38 MAP kinase pathways, and inhibition of mTOR and p38 MAP kinase allowed LC3-II induction in glutamine-deprived cells. Under glutamine starvation, LC3-II recovery after heat stress or the increase under oxidative stress was blunted significantly. Glutamine depletion increased caspase-3 and poly (ADP-ribose) polymerase activity after heat stress, which was inhibited by treatment with inhibitors of mTOR and p38 MAP kinase. **Conclusions:** Glutamine induces autophagy under basal and stressed conditions, and prevents apoptosis under heat stress through its regulation of the mTOR and p38 MAP kinase pathways. We propose that glutamine contributes to cell survival during physiologic stress by induction of autophagy.

Glutamine is the most abundant free amino acid in the body and is a major respiratory fuel and metabolic precursor for many cell types including intestinal epithelial cells (IECs) and immune cells.^{1–3} Although considered nonessential, glutamine becomes conditionally essential during severe catabolic stress such as major surgery, trauma, or sepsis in which intracellular and plasma glutamine levels decrease rapidly.^{4,5} Recent studies have shown supplementation of parenteral or

enteral glutamine reduces complication rates in critically ill and postoperative patients.^{6–8}

The mechanisms underlying glutamine's protective and trophic actions are incompletely understood. The possibility that it might be essential for the autophagic response of intestinal epithelial cells was therefore considered by this study. Autophagy is a catabolic process that recycles cellular proteins and organelles, an evolutionarily conserved response to metabolic stress.^{9–11} Autophagy is recognized as a cell survival mechanism during periods of nutrient deprivation in which the bulk degradation of cytoplasmic proteins and nonessential organelles provides an alternative energy source. The process of autophagy is characterized by the formation of double-membrane vesicles known as autophagosomes, which is mediated by the Atg12-Atg5-Atg16 complex and microtubule-associated protein light chain 3 (LC3)-phospholipid conjugates (LC3-II).^{12,13} The outer membrane of the autophagosome fuses with the lysosome, and cytoplasm-derived materials are degraded in autolysosome.

Amino acids have long been known to be regulators of autophagy.¹⁴ The signaling mechanism by which amino acids regulate autophagy appears to involve stimulation of mammalian target of rapamycin (mTOR) kinase,^{15–17} although recent studies showed that they also may use mTOR-independent pathways.^{18,19} Only certain amino acids are capable of modulating autophagy and their actions are highly cell-specific.²⁰

In the present study, we show that glutamine induces autophagy in rat intestinal epithelial IEC-18 cells and human colonic epithelial Caco-2_{BBE} cells, a process that is mediated by inhibition of the mTOR and p38 mitogen-activated protein (MAP) kinase pathways. In IEC-18 cells, glutamine also maintains autophagy under heat- and oxidative-stressed conditions and prevents apoptosis under heat-stressed conditions. Our data suggest that glutamine contributes to cell survival during

Abbreviations used in this paper: BBE, brush border expression; DMEM, Dulbecco's modified Eagle medium; Hsp, heat shock protein; IEC, intestinal epithelial cell; LC3, microtubule-associated protein light chain 3; MAP, mitogen-activated protein; mTOR, mammalian target of rapamycin; PARP, poly (ADP-ribose) polymerase; SAPK, stress-activated protein kinase; siRNA, short interfering RNA; S6K, p70 S6 kinase; TBS, Tris-buffered saline; TBST, Tris-buffered saline with Tween.

© 2009 by the AGA Institute

0016-5085/09/\$36.00

doi:10.1053/j.gastro.2008.12.002

physiologic stress by induction of autophagy through its regulation of the mTOR and p38 MAP kinase pathways.

Materials and Methods

Chemicals

Chemicals were obtained from Fisher Scientific (Hanover Park, IL) unless otherwise stated. Media and all cell culture supplements were obtained from Invitrogen (Grand Island, NY), L-leucine and 3-methyladenine were obtained from Sigma-Aldrich (St. Louis, MO), and rapamycin and SB203580 were obtained from Axxora (San Diego, CA).

Cell Culture

The diploid nontransformed rat small intestinal epithelial IEC-18 cell line (ATCC, Manassas, VA; CRL-1589) was used between passages 20 and 35. IEC-18 cells were grown in high-glucose (4.5 g/L) Dulbecco's modified Eagle medium (DMEM) containing 2 mmol/L L-glutamine, 5% vol/vol fetal bovine serum, 50 U/mL penicillin, 50 μ g/mL streptomycin, and 0.1 U/mL insulin, and cultured to 90% confluence. The human colon carcinoma cell line Caco-2_{BBE} (brush border expressor) was used between passages 50 and 75. Caco-2_{BBE} cells were seeded onto cell culture inserts at a density of 10^5 cells/cm², grown in high-glucose DMEM containing 2 mmol/L L-glutamine, 10% vol/vol fetal bovine serum, 50 U/mL penicillin, 50 μ g/mL streptomycin, and 10 μ g/mL transferrin, and allowed to differentiate for 14 days. Both cell lines then were incubated for 24 hours in reduced-serum (1% vol/vol fetal bovine serum) DMEM containing indicated concentrations of glutamine with all other supplements. Cell cultures were maintained in a humidified 5% CO₂ incubator at 37°C. Heat shock was achieved by sealing dishes and immersing them in a 42°C water bath for 15 or 30 minutes. For confocal microscopy, cells were grown in complete growth medium on glass coverslips. IEC-18 cells were cultured to 90% confluence, and Caco-2_{BBE} cells were cultured for 14 days. Cells then were incubated for 24 hours in reduced-serum DMEM containing either 0 or 0.7 mmol/L glutamine with all other supplements.

RNA Silencing of mTOR and p38 MAP Kinase

To silence mTOR or p38 MAP kinase, predesigned short interfering RNA (siRNA) specific for rat mTOR (NM_019906, bases 710–728, ID number: 132719) or p38 MAP kinase (NM_031020, bases 666–684, ID number: 135448) were purchased from Ambion (Austin, TX). As a negative control, AllStars Negative Control siRNA (Qiagen, Valencia, CA) was used. siRNA (final concentration, 5 nmol/L) was mixed with siLentFect lipid reagent (Bio-Rad, Hercules, CA) in Opti-MEM (Invitrogen) and allowed to form complexes for 30 minutes at room temperature. Complexes were added to 70% confluent IEC-18 cells, in which 15 minutes earlier the complete medium had been replaced with Opti-MEM. The cells were incubated at 37°C for 30

minutes and then complete medium with 10% vol/vol fetal bovine serum was added. Twenty-four hours after the transfection, cells were incubated for 24 hours in reduced-serum DMEM without glutamine.

Western Blot Analysis

Cells were scraped and disrupted in lysis buffer (composition: 50 mmol/L Tris pH 7.4, 150 mmol/L NaCl, 1% vol/vol NP-40, 1 mmol/L Na₃VO₄, 1 mmol/L NaF, and the complete protease inhibitor cocktail [Roche Molecular Biosciences, Indianapolis, IN]). An aliquot was removed and protein concentrations were measured using bicinchoninic acid. Laemmli sample buffer was added to the remainder (composition: 250 mmol/L Tris pH 7.4, 2% wt/vol sodium dodecyl sulfate, 25% vol/vol glycerol, 10% vol/vol 2-mercaptoethanol, and 0.01% wt/vol bromophenol blue) and samples were heated to 70°C for 10 minutes and stored at –80°C until analysis. Equal amounts of protein were separated by sodium dodecyl sulfate–polyacrylamide gel electrophoresis and transferred immediately onto polyvinylidene difluoride membranes (Polyscreen; Perkin-Elmer, Boston, MA) using 1× Towbin buffer (25 mmol/L Tris pH 8.8, 192 mmol/L glycine, 15% vol/vol methanol). Membranes subsequently were incubated in 3% wt/vol bovine serum albumin in Tris-buffered saline (TBS with Tween [TBST]; composition: 140 mmol/L NaCl, 5 mmol/L KCl, 10 mmol/L Tris pH 7.4, with 0.1% vol/vol Tween 20) at room temperature for 1 hour. Antibodies were added and incubated overnight at 4°C in TBST. Polyclonal rabbit antibodies against LC3 (2775), phospho-mTOR (2971), mTOR (2972), phospho-p70 S6 kinase (9205), phospho-p38 MAP kinase (9211), p38 MAP kinase (9212), phospho-p44/42 MAP kinase (extracellular signal-related kinase) (9101), phospho-SAPK (stress-activated protein kinase)/c-Jun amino-terminal kinase (9251), caspase-3 (9662) and poly (ADP-ribose) polymerase (PARP) (9542), and monoclonal mouse antibody against phospho-Akt (4051) were purchased from Cell Signaling (Danvers, MA). Polyclonal rabbit antibody against heat shock protein (Hsp)25 (SPA-801) and monoclonal mouse antibody against Hsp70 (SPA-810) were purchased from Stressgen/Assay Designs (Ann Arbor, MI). Monoclonal mouse antibody against β -actin (AAN01) was purchased from Cytoskeleton (Denver, CO). Membranes were washed 3 times in TBST and subsequently incubated with species-appropriate, peroxidase-conjugated secondary antibodies (1 h; Jackson ImmunoResearch, West Grove, PA). Blots were washed 3 times with TBST and once with TBS without Tween and developed using an enhanced chemiluminescence system (Supersignal; Pierce Chemical, Rockford, IL).

Confocal Microscopy of Autophagosomes

After treatment with 0 or 0.7 mmol/L glutamine in reduced-serum DMEM for 24 hours, cells were washed in phosphate-buffered saline (PBS) and then fixed with 4% paraformaldehyde (Electron Microscopy Sciences, Hatfield,

PA) for 15 minutes at room temperature. Fixed cells were washed with PBS, permeabilized in 100% methanol for 10 minutes at -20°C , washed in PBS, and blocked in blocking buffer (X909; DAKO, Carpinteria, CA) for 1 hour at room temperature. Cells subsequently were incubated with anti-LC3 antibody in antibody diluent (S3022; DAKO) for overnight at 4°C . After 3 TBST washes, cells were incubated with Cy2-anti-rabbit antibody (Jackson ImmunoResearch) in antibody diluent for 2 hours at room temperature and then washed 3 times in TBST. Coverslips were mounted on slides using SlowFade Gold antifade reagent with 4',6-diamidino-2-phenylindole (Invitrogen). Cells were observed with a Leica TCS SP2 Laser Scanning Confocal Microscope, photographed at a magnification of 400 \times , and analyzed using Leica Confocal Software (Leica Microsystems Inc, Bannockburn, IL).

Data Analysis

All experiments were repeated at least 3 times with cells of different passage numbers. Densitometry of autoradiography images was performed using ImageJ (Research Services Branch, National Institute of Mental Health, Bethesda, MD) and normalized to the signal intensity of β -actin for equal protein loading control for each sample in each experiment. This quantitation was performed within the linear range of the standard curve defined by the standard sample, β -actin, for all densitometry analysis. For confocal microscopy experiments, the number of LC3 punctate dots and nuclei were counted using ImageJ software. Statistical analysis (analysis of variance [ANOVA]) was performed by using a Bonferroni correction with StatView 5.0 (SAS Institute, Cary, NC). Data were expressed as means \pm SE.

Results

Glutamine Increases Autophagy in IEC-18 and Caco-2_{BBE} Cells

Autophagosome formation is a complex, multistage process that involves many proteins.⁹⁻¹¹ The process can be assessed most readily by following the phospholipid conjugation of the protein LC3-I (cytosolic form) to LC3-II (autophagosomal membrane-bound form), which has an increased gel mobility on sodium dodecyl sulfate-polyacrylamide gel electrophoresis.^{12,13} Autophagosome formation also can be visualized because LC3-II accumulates in this organelle. To determine if glutamine is required for autophagosome formation, IEC-18 and Caco-2_{BBE} cells were incubated with varying concentrations of glutamine for 24 hours. The concentration range of glutamine ranged from the physiologic concentration normally found in plasma (0.7 mmol/L) to concentrations that were pharmacologic (2.8 mmol/L). In the absence of glutamine, a small degree of LC3-II expression could be detected by Western blotting (Figure 1A and B), which additionally was reflected by a small number of autophagosomes observed by confocal microscopy (Figure

1C and D). However, with increasing glutamine concentration, a significant increase in both the phospholipid-conjugated LC3-II as well as the number of autophagosomes is observed (Figure 1A-D, autophagosome number quantified in Figure 1E and F).

Glutamine is essential for the metabolic and nutritional status of the intestinal epithelial cell,² but other amino acids also play a role in this regard. For instance, leucine is believed to be a potent inhibitor of autophagy.¹⁵⁻¹⁷ Therefore, we examined the effects of leucine on glutamine-stimulated autophagy (supplementary Figure 1; see supplementary material online at www.gastrojournal.org). Because the concentration of leucine in DMEM is 0.8 mmol/L, this concentration was defined as *basal* in assessing LC3-II expression. IEC-18 and Caco-2_{BBE} cells were treated for 24 hours with varying concentrations of leucine (0.8-6.4 mmol/L) with or without 0.7 mmol/L glutamine. Doubling the leucine concentration to 1.6 mmol/L reduced glutamine's induction of LC3-II by approximately 20% in both cells and increasing leucine further caused an even greater inhibition of glutamine LC3-II induction (supplementary Figure 1; see supplementary material online at www.gastrojournal.org).

Leucine has been shown to alter the activity of a number of proteins in the cell including mTOR.²⁰ mTOR is a kinase that phosphorylates a number of targets, including p70 S6 kinase (S6K). Because Akt (protein kinase B) is a serine/threonine kinase that regulates the activity of mTOR, we used phospho-specific antibodies to examine states of activation of Akt, mTOR, and S6K in conditions of glutamine starvation. Within 6 hours of glutamine depletion, LC3-II decreased, paralleled by increases in phosphorylated Akt, mTOR, and S6K in IEC-18 and Caco-2_{BBE} cells (Figure 2A and B).

The identical samples also were analyzed for activation of certain MAP kinases because they also could be involved in the regulation of the autophagic response. In the presence of glutamine, p38 MAP kinase showed a low level of phosphorylation that increased within 6 hours of glutamine deprivation (Figure 2A and B), suggesting a role of glutamine to regulate this kinase. Minimal to no changes were observed in phosphorylation of extracellular signal-related kinase or c-Jun amino-terminal kinase upon glutamine deprivation (data not shown).

To confirm the role of mTOR and p38 MAP kinase in glutamine induction of LC3-II, pharmacologic inhibitors of mTOR (rapamycin) and p38 MAP kinase (SB203580), or siRNAs for mTOR and p38 MAP kinase, were used in IEC-18 cells. As previously shown, glutamine depletion decreased the level of LC3-II, which was paralleled by an activation of mTOR and p38 MAP kinase (Figure 3). Treatment of the cells with rapamycin (100 nmol/L for 24 hours) and SB203580 (5 $\mu\text{mol/L}$ for 24 hours) leads to the induction of LC3-II, even under conditions of glutamine depletion. Silencing mTOR and p38 MAP kinase also restored LC3-II to near-normal levels in glutamine-deprived cells.

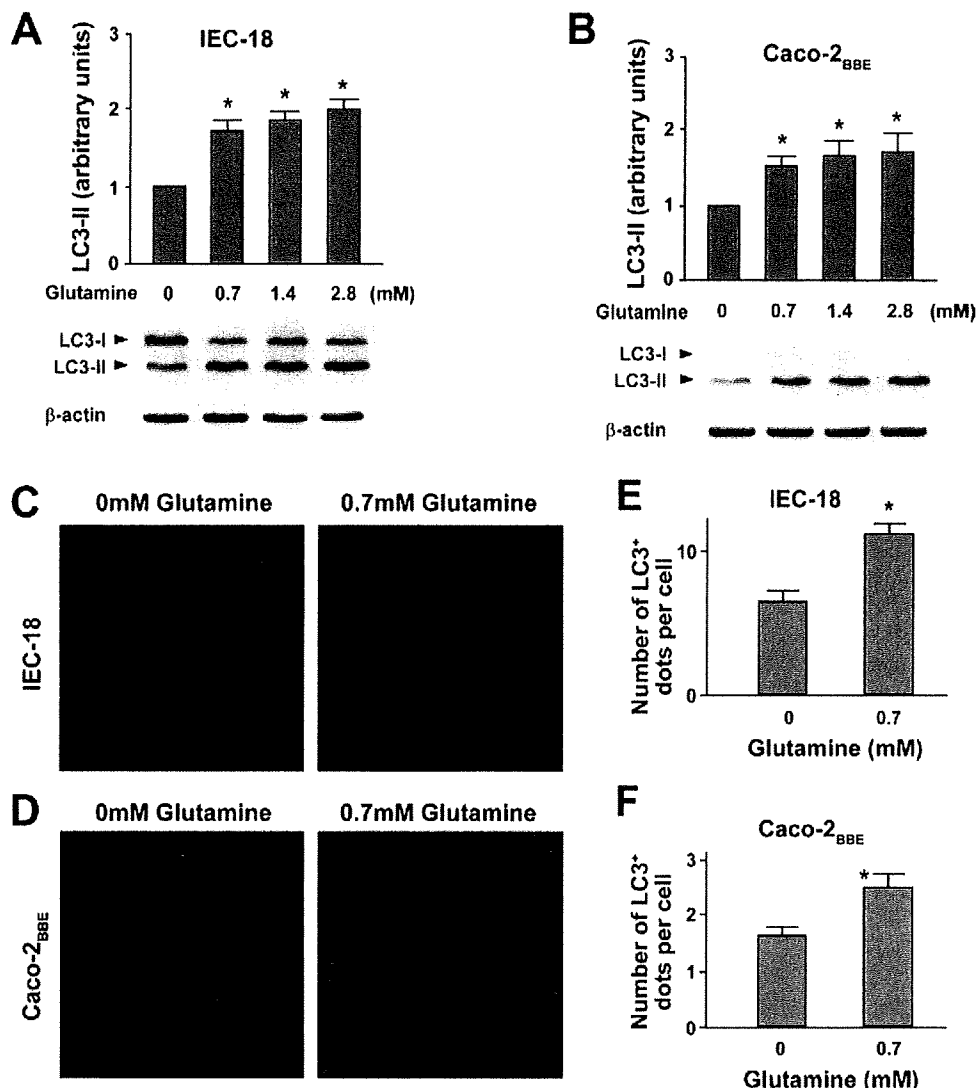


Figure 1. Glutamine enhances autophagy in IEC-18 and Caco-2_{BBE} cells. (A) IEC-18 cells were incubated with varying concentrations of glutamine for 24 hours and analyzed by Western blotting. The ratio of LC3-II to β -actin density was calculated using ImageJ software and set to 1 for the glutamine-deprived condition. Images are representative of 4 separate experiments. (B) Caco-2_{BBE} cells were incubated with varying concentrations of glutamine for 24 hours and analyzed by Western blotting. The ratio of LC3-II to β -actin density was calculated using ImageJ software and set to 1 for glutamine-deprived conditions. Images are representative of 4 separate experiments. (C) Autophagosome formation in IEC-18 cells was observed using confocal microscopy in the absence and presence of glutamine. IEC-18 cells were incubated with 0 or 0.7 mmol/L glutamine for 24 hours, fixed, and stained for LC3 (green), and nuclei were stained using 4',6-diamidino-2-phenylindole (blue). Images are representative of 3 separate experiments. (D) Autophagosome formation in Caco-2_{BBE} cells was observed using confocal microscopy in the absence and presence of glutamine. Caco-2_{BBE} cells were incubated with 0 or 0.7 mmol/L glutamine for 24 hours, fixed, and stained for LC3 (green), and nuclei were stained using 4',6-diamidino-2-phenylindole (blue). Images are representative of 3 separate experiments. Autophagosome formation, visualized by accumulation of LC3, was quantified and counted using ImageJ software in at least 300 cells in each experiment. Shown are the (E) number of autophagosomes per cell of IEC-18 cells, and the (F) number of Caco-2_{BBE} cells. Data are shown as means \pm SE. * $P < .05$ compared with 0 mmol/L glutamine by ANOVA using a Bonferroni correction.

Therefore, both the mTOR and p38 MAP kinase pathways appear to be involved in the regulation of autophagy by glutamine.

Glutamine Maintains Autophagy and Inhibits Apoptosis Under Stressed Conditions

Autophagy may play a role in cellular maintenance and protection, particularly under conditions of stress.²¹ We

therefore examined glutamine-dependent autophagic responses in cells subjected to thermal (heat) stress, a physiologic equivalent of fever. To determine if heat stress promotes an autophagic response, IEC-18 cells (grown in 0.7 mmol/L glutamine) were subjected to 42°C for up to 30 minutes. As shown in Figure 4A, heat stress caused a significant decrease in LC3-II, but, after heat stress and during

BASIC-ALIMENTARY TRACT

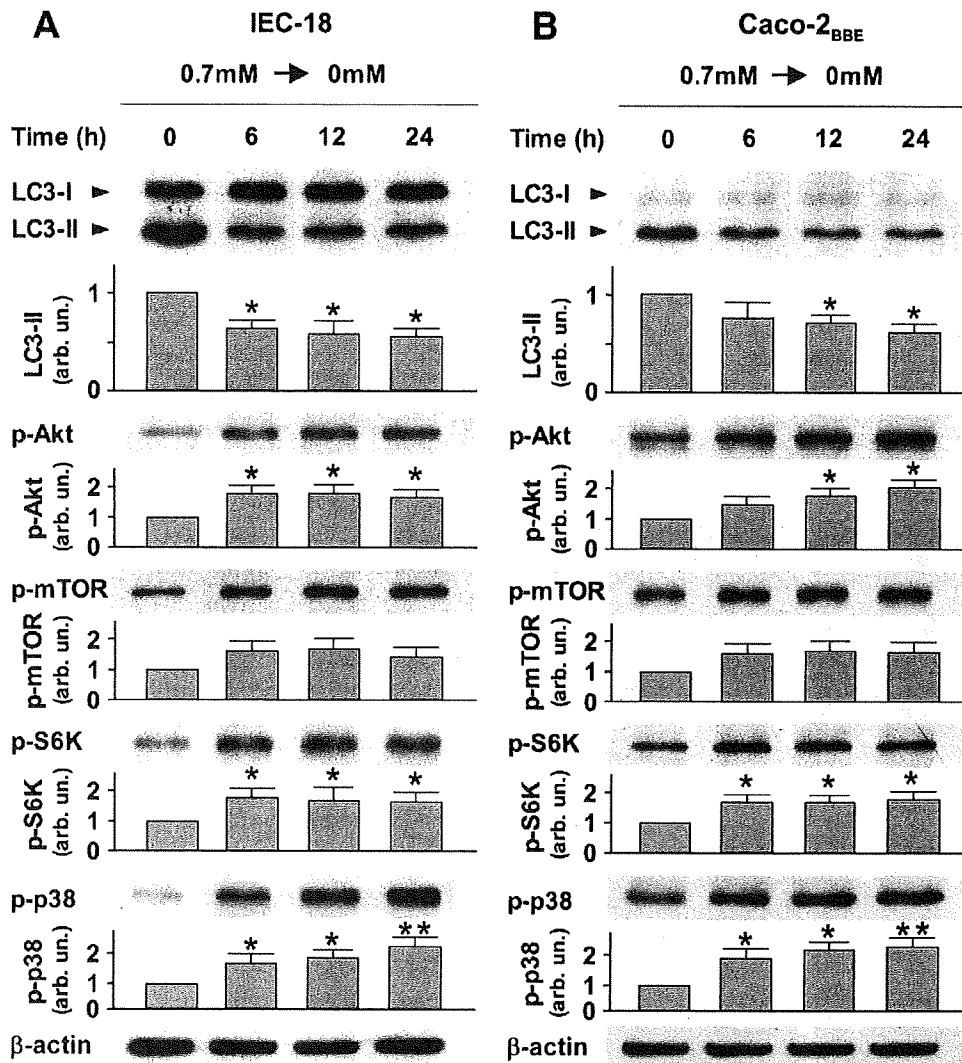


Figure 2. Glutamine inhibits mTOR and p38 MAP kinase activity in IEC-18 and Caco-2_{BBE} cells. (A) IEC-18 cells were incubated with 0.7 mmol/L glutamine for 24 hours. Cells subsequently were deprived of glutamine for varying times up to 24 hours. Samples were collected at designated times and analyzed by Western blotting. Images are representative of 3 separate experiments. (B) Caco-2_{BBE} cells were incubated with 0.7 mmol/L glutamine for 24 hours. Cells subsequently were deprived of glutamine for varying times up to 24 hours. Samples were collected at designated times and analyzed by Western blotting. Images are representative of 3 separate experiments. Densitometric values were obtained using ImageJ software and normalized to β -actin, set to 1 for conditions immediately after glutamine deprivation (0 hour). Data are shown as means \pm SE. * $P < .05$ and ** $P < .01$ compared with cells at time point 0 hour by ANOVA using a Bonferroni correction.

the recovery phase (37°C), this response attenuated and LC3-II abundance returned back to normal levels. Heat stress also stimulated phosphorylation of Akt and mTOR, the latter to a lesser extent. Both changes returned to a near-basal state after the heat stress removal during the recovery phase. The activity of p38 MAP kinase and expression of β -actin were not affected by heat stress. The induction of Hsp70 and Hsp25, 2 known heat-inducible stress proteins, could be seen clearly during the recovery phase. To determine if mTOR is responsible for the regulation of autophagy by heat stress, cells were pretreated with rapamycin (100 nmol/L for 24 hours). Rapamycin-treated cells did not show the LC3-II decrease during heat or the LC3-II increase upon return to 37°C (Figure 4B).

To determine whether glutamine plays a role in the autophagy response to heat stress, cells were incubated for 24 hours with 0.7 or 0 mmol/L glutamine. Under conditions of glutamine depletion, the autophagy response to heat stress was minimal and the LC3-II increase after heat stress was small, despite inactivation of mTOR (Figure 5A). In con-

trast, the robust activation of p38 MAP kinase in glutamine-deprived cells led us to postulate that p38 MAP kinase activation might be involved in inhibition of the normal autophagy response to heat stress. To test this hypothesis, glutamine-deprived cells were treated with the p38 MAP kinase inhibitor SB203580 (5 μ mol/L for 24 hours). Treatment with SB203580 restored the LC3-II levels under basal as well as heat-stressed conditions (Figure 5B). Moreover, the changes of LC3-II levels during heat and after heat were similar to those in glutamine-treated cells (compare 0.7 mmol/L glutamine in Figure 5A with 0 mmol/L + SB203580 in Figure 5B). These results suggest that glutamine regulates autophagy by suppression of p38 MAP kinase activity under heat-stressed conditions.

We also examined the glutamine-dependent autophagic responses to oxidative stress (supplementary Figure 2; see supplementary material online at www.gastrojournal.org). When glutamine was present, 500 μ mol/L H₂O₂ caused a significant increase in LC3-II, paralleled by a decrease in

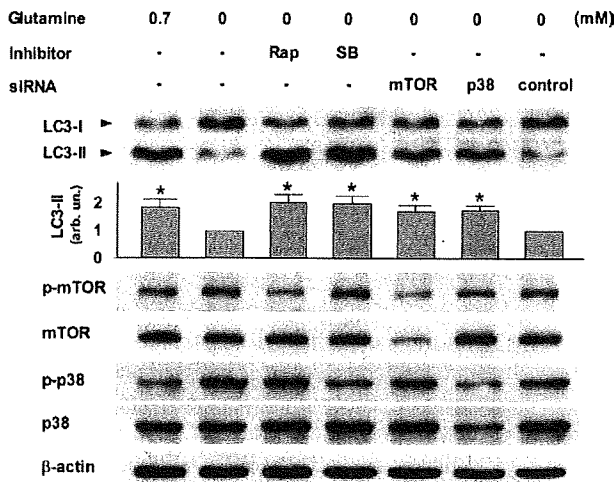


Figure 3. mTOR and p38 MAP kinase pathways are involved in glutamine's regulation of autophagy in IEC-18 cells. IEC-18 cells were incubated in 0.7 mmol/L glutamine-supplemented medium for 24 hours, or glutamine-deprived media without or with mTOR inhibitor rapamycin (Rap; 100 nmol/L) and p38 MAP kinase inhibitor SB203580 (SB; 5 μmol/L) for 24 hours. For silencing of mTOR and p38 MAP kinase with siRNA, silencing oligonucleotides or nonsilencing siRNA (control) were introduced into 70% confluent IEC-18 cells. Twenty-four hours after the transfection, cells were incubated for 24 hours in glutamine-deprived media. Total cell lysates were analyzed by Western blotting. Images are representative of 3 separate experiments. The ratio of LC3-II to β-actin density was calculated using ImageJ software, and set to 1 for no glutamine, inhibitors, and siRNA. Data are shown as means ± SE. **P* < .05 compared with 0 mmol/L glutamine, no inhibitors, and siRNA by ANOVA using a Bonferroni correction.

phosphorylated mTOR. However, treatment with H₂O₂ stimulated the phosphorylation of p38 MAP kinase. Under glutamine deprivation, H₂O₂-induced LC3-II increase was minimal, as in the case of heat stress. In the absence of glutamine and despite decreased phosphorylation of mTOR after the addition of H₂O₂, p38 MAP kinase showed a strong activation (supplementary Figure 2A; see supplementary material online at www.gastrojournal.org). The restoration of the LC3-II level by the treatment with SB203580 (5 μmol/L for 24 hours) in glutamine-deprived cells suggests that glutamine also increases autophagy under oxidative stressed conditions through its inhibitory effect on p38 MAP kinase (supplementary Figure 2B; see supplementary material online at www.gastrojournal.org).

Heat stress can potentially stimulate an apoptotic response, but could depend on the metabolic state of the cell. In support of this, in the absence of glutamine, heat stress increased the production of cleaved caspase-3, a pivotal asparagine protease in the apoptotic response, and cleaved PARP, one of the main cleavage targets of caspase-3 (Figure 6, middle lane). Glutamine supplementation decreased cleaved caspase-3 and PARP (0.7 mmol/L; Figure 6, far left lane), indicating the presence of glutamine can direct cell fate and prevent apoptosis during heat stress recovery. Also notable is that when autophagy was blocked with 3-methyladenine

(10 mmol/L for 24 hours) in glutamine-supplemented condition, cleaved caspase-3 and PARP increased, suggesting that in the absence of the autophagic response the cell defaults to apoptosis under conditions of heat stress. To

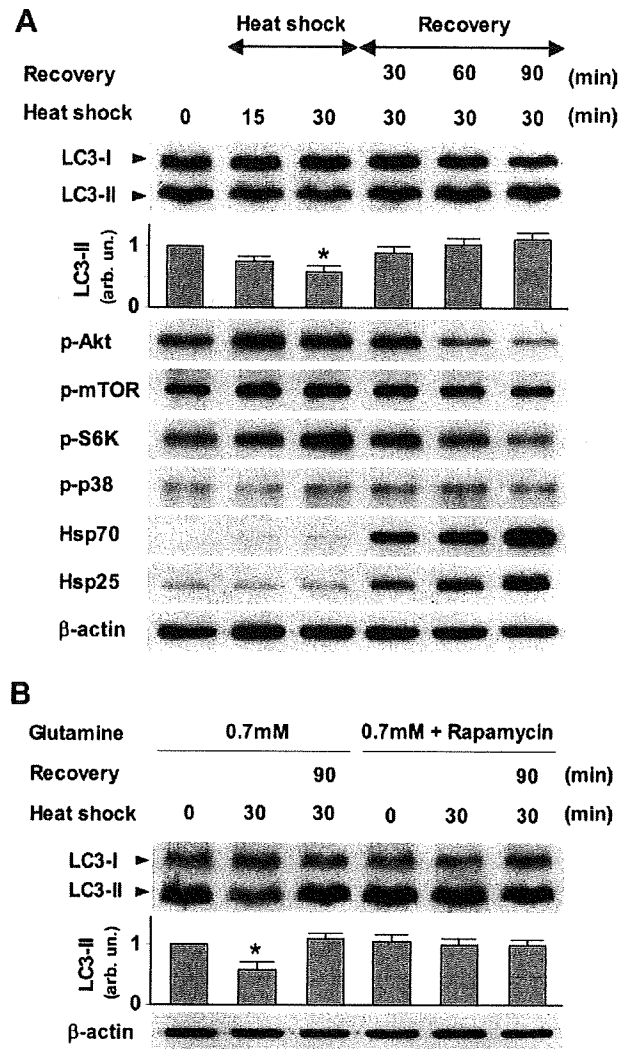


Figure 4. Heat stress regulates autophagy via the mTOR pathway. (A) IEC-18 cells were incubated with 0.7 mmol/L glutamine for 24 hours followed by heat shock at 42°C for 15 or 30 minutes, collected at designated times, and analyzed by Western blotting. The ratio of LC3-II to β-actin density was calculated using ImageJ software, set to 1 for the sample before heat shock. Images are representative of 3 separate experiments. Data are shown as means ± SE. **P* < .05 compared with unstimulated conditions by ANOVA using a Bonferroni correction. (B) Inhibition of the mTOR pathway blocks the autophagy response to heat stress. IEC-18 cells were incubated in 0.7 mmol/L glutamine-supplemented media without rapamycin (3 left lanes) or with 100 nmol/L rapamycin (3 right lanes) for 24 hours followed by heat shock at 42°C for 30 minutes. Cells were collected before, immediately after, and 90 minutes after heat shock, and analyzed by Western blotting. The ratio of LC3-II to β-actin density was calculated using ImageJ software, set to 1 for unstimulated conditions without rapamycin. Images are representative of 3 separate experiments. Data are shown as means ± SE. **P* < .05 compared with unstimulated conditions and no rapamycin by ANOVA using a Bonferroni correction.

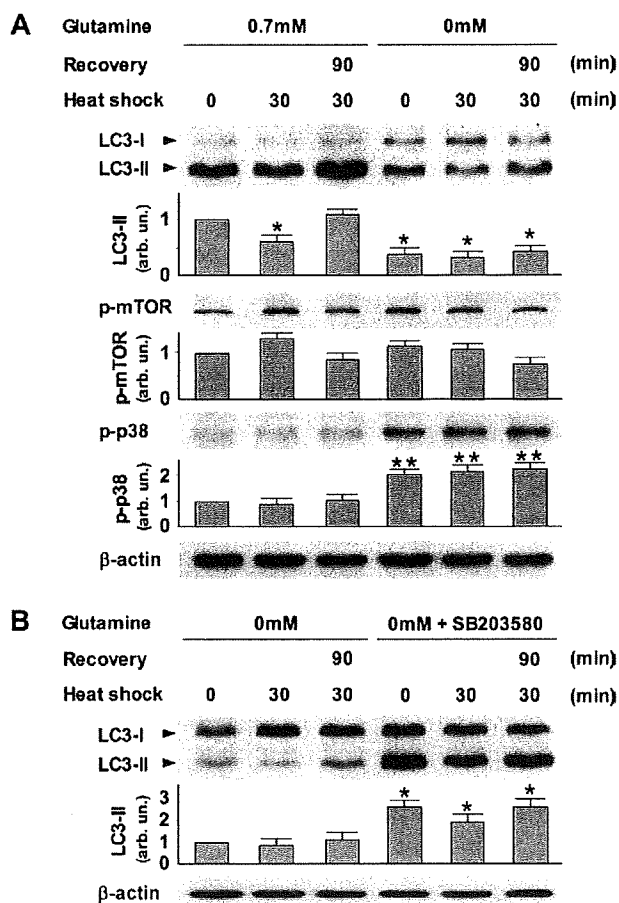


Figure 5. Glutamine depletion decreases the autophagy response to heat stress by the activation of p38 MAP kinase. (A) Decreased autophagy response to heat stress in glutamine-depleted cells. IEC-18 cells were incubated with 0.7 mmol/L glutamine (3 left lanes) or without glutamine (3 right lanes) for 24 hours followed by heat shock at 42°C for 30 minutes. Cells were collected before, immediately after, and 90 minutes after heat shock, and analyzed by Western blotting. Images are representative of 3 separate experiments. Densitometric values were obtained using ImageJ software and normalized to β -actin, set to 1 for unstimulated conditions in 0.7 mmol/L glutamine. Data are shown as means \pm SE. * P < .05 and ** P < .01 compared with unstimulated conditions and 0.7 mmol/L glutamine by ANOVA using a Bonferroni correction. (B) Inhibition of p38 MAP kinase restores the normal autophagy response to heat stress in glutamine-depleted cells. IEC-18 cells were incubated in glutamine-depleted media without SB203580 (3 left lanes) or with 5 μ mol/L SB203580 (3 right lanes) for 24 hours followed by heat shock at 42°C for 30 minutes. Cells were collected before, immediately after, and 90 minutes after heat shock, and analyzed by Western blotting. Images are representative of 3 separate experiments. The ratio of LC3-II to β -actin density was calculated using ImageJ software, and set to 1 for unstimulated conditions without glutamine and SB203580. Data are shown as means \pm SE. * P < .05 compared with unstimulated conditions, 0 mmol/L glutamine, and no SB203580 by ANOVA using a Bonferroni correction.

determine the involvement of mTOR and p38 MAP kinase, glutamine-depleted cells were treated with rapamycin or SB203580 (100 nmol/L or 5 μ mol/L, respectively) for 24 hours. Both rapamycin and SB203580 inhibited the forma-

tion of cleaved caspase-3 and PARP under glutamine-depleted, heat-stressed conditions (Figure 6, 2 right lanes). Thus, these inhibitors restore the autophagy response even under glutamine-depleted conditions, supporting the notion of a balance between the autophagy and apoptotic responses in IEC-18 cells that is dependent on glutamine and regulation of mTOR and p38.

Discussion

The gut mucosa continually faces physiologic stresses, including large changes in luminal pH and osmolarity, luminal bacteria, and physiologic state of immune and inflammatory activation.²² Several factors are important in maintaining gut homeostasis. Glutamine, for example, may regulate proliferation of intestinal epithelial cells by modulating responsiveness to growth factors.^{23,24} Small intestinal mucosa becomes atrophic when the gut is deprived of glutamine, as occurs during total parenteral nutrition.²⁵ Glutamine depletion can increase permeability of the gut, which promotes translocation of luminal bacteria and toxins.²⁶ Glutamine has been shown to protect intestinal epithelial cells during physiologic stress because it is required for stress-induced Hsp expression.^{27,28} It also has been shown to attenuate cytokine expression as well as nuclear factor κ B activation,²⁹⁻³¹ enhance glutathione synthesis,³² and prevent apoptosis.³³⁻³⁵

Autophagy generally is considered a survival process during periods of metabolic stress.^{36,37} However, more re-

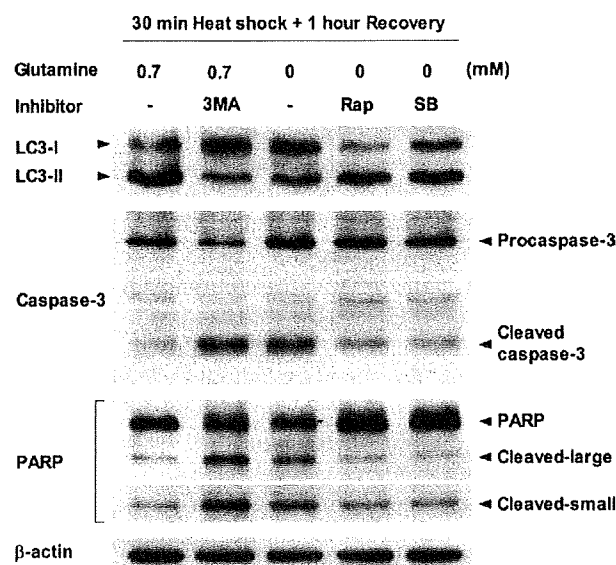


Figure 6. Enhanced autophagy decreases apoptosis in IEC-18 cells. IEC-18 cells were incubated in 0.7 mmol/L glutamine-supplemented media without or with 3-methyladenine (3 MA; 10 mmol/L) for 24 hours (2 left lanes), or incubated in glutamine-depleted media without or with rapamycin (Rap; 100 nmol/L) and SB203580 (SB; 5 μ mol/L) for 24 hours (3 right lanes). The cells were heat shocked at 42°C for 30 minutes, followed by a 1-hour recovery, and analyzed by Western blotting. Images are representative of 3 separate experiments. β -actin was used as a loading control.

cently, its role as a survival pathway under other forms of stress, including oxidative and toxic (anticancer drug), has become increasingly recognized.^{21,38} Autophagy also plays a role in clearing intracellular microbes and bacterial toxins.^{39,40} Polymorphisms of 2 related autophagy genes, ATG16L1 and IRGM, were shown to be associated with an increased risk for inflammatory bowel diseases.^{41–43} When ATG16L1 and IRGM expression were silenced by siRNA, cellular ability to form autophagosomes was compromised, as was autophagic clearance of *Salmonella typhimurium* and *Mycobacteria*, respectively.^{42,44} In this study, we show that glutamine is essential for autophagy in intestinal epithelial cells. Glutamine depletion, on the other hand, compromises this process, both under basal and stressed conditions, and, in the latter case, cell fate defaults to apoptosis.

Several cell signaling pathways are involved in the regulation of autophagy, which are cell type-specific and signal-dependent.⁴⁵ mTOR is involved in the negative control of autophagy and has been proposed as a nutrient sensor, although the way by which amino acids, leucine in particular, modulate mTOR activity is not fully understood.²⁰ In rat hepatocytes, glutamine is able to activate p70 S6K, a downstream target of mTOR, alone or in combination with leucine.⁴⁶ By contrast, glutamine reverses the activation of p70 S6K induced by leucine in IEC-18 cells.⁴⁷ Antagonistic effects of leucine and glutamine on the mTOR pathway also have been reported in myogenic C₂C₁₂ cells.⁴⁸ Likewise, glutamine's effects on p38 MAP kinase vary depending on the cell type. Glutamine induces p38 MAP kinase activation in rat hepatocytes,⁴⁹ but in IEC-18 and Caco-2_{BBE} cells, it inhibits p38 MAP kinase activity. The role of the p38 MAP kinase as a negative regulator of autophagy also has been described in hepatocytes after stimulation by insulin, ethanol, and amino acids such as glutamine and glycine,⁴⁹ and induction of autophagy by inhibition of the p38 MAP kinase pathway recently was reported in colorectal cancer cells.⁵⁰

We believe our study has several important clinical implications. Under conditions of critical illness, postsurgical stress, chronic inflammation, or starvation, glutamine is depleted rapidly from the body.^{4,5} Organs such as the gastrointestinal tract, which are highly dependent on glutamine as a fuel source, are particularly susceptible to injury under these conditions. If sustained, glutamine depletion could impair the gut's ability to mount an autophagic response. That would have at least 2 potential complications. First, the inability to mount an autophagic response could increase mucosal injury to stress (heat [fever], oxidant [ischemia-reperfusion], and so forth), resulting in increased cellular apoptosis, enhanced mucosal permeability, and dysfunction of transport mechanisms. This could explain the observed transmigration of luminal organisms and microbial-derived products such as lipopolysaccharide and peptidoglycan. Second, impairment of autophagy could impair normal clearance of intracellular organisms or enterotoxins, particularly opportunistic infectious pathogens.^{40,42,44} We

speculate that this may contribute to the poor outcomes and increased susceptibility of malnourished populations during epidemics of infectious diarrheal diseases.

In summary, we report that glutamine is essential for maintaining autophagy and mounting an autophagic response under conditions of stress in intestinal epithelial cells. A model for glutamine regulation of autophagy is shown in supplementary Figure 3 (see supplementary material online at www.gastrojournal.org). Under conditions of glutamine depletion, IECs are unable to mount an autophagic response to stress, resulting in apoptosis. Glutamine contributes to cell survival during physiologic stress by induction of autophagy through its regulation of the mTOR and p38 MAP kinase pathways.

Supplementary Data

Note: To access the supplementary material accompanying this article, visit the online version of *Gastroenterology* at www.gastrojournal.org, and at doi: 10.1053/j.gastro.2008.12.002.

References

- Stein WH, Moore S. The free amino acids of human blood plasma. *J Biol Chem* 1954;21:915–926.
- Windmueller HG, Spaeth AE. Respiratory fuels and nitrogen metabolism in vivo in small intestine of fed rats. Quantitative importance of glutamine, glutamate, and aspartate. *J Biol Chem* 1980;255:107–112.
- Newsholme P. Why is L-glutamine metabolism important to cells of the immune system in health, postinjury, surgery or infection? *J Nutr* 2001;131:2515S–2522S.
- Askanazi J, Carpentier YA, Michelsen CB, et al. Muscle and plasma amino acids following injury. Influence of intercurrent infection. *Ann Surg* 1980;192:78–85.
- Parry-Billings M, Evans J, Calder PC, et al. Does glutamine contribute to immunosuppression after major burns? *Lancet* 1990;336:523–525.
- Goeters C, Wenn A, Mertes N, et al. Parenteral L-alanyl-L-glutamine improves 6-month outcome in critically ill patients. *Crit Care Med* 2002;30:2032–2037.
- Novak F, Heyland DK, Avenell A, et al. Glutamine supplementation in serious illness: a systematic review of the evidence. *Crit Care Med* 2002;30:2022–2029.
- Griffiths RD, Allen KD, Andrews FJ, et al. Infection, multiple organ failure, and survival in the intensive care unit: influence of glutamine-supplemented parenteral nutrition on acquired infection. *Nutrition* 2002;18:546–552.
- Levine B, Klionsky DJ. Development by self-digestion: molecular mechanisms and biological functions of autophagy. *Dev Cell* 2004;6:463–477.
- Ohsumi Y. Molecular dissection of autophagy: two ubiquitin-like systems. *Nat Rev Mol Cell Biol* 2001;2:211–216.
- Klionsky DJ, Emr SD. Autophagy as a regulated pathway of cellular degradation. *Science* 2000;290:1717–1721.
- Kabeya Y, Mizushima N, Ueno T, et al. LC3, a mammalian homologue of yeast Apg8p, is localized in autophagosome membranes after processing. *EMBO J* 2000;19:5720–5728.
- Tanida I, Minematsu-Ikeguchi N, Ueno T, et al. Lysosomal turnover, but not a cellular level, of endogenous LC3 is a marker for autophagy. *Autophagy* 2005;1:84–91.

14. Schworer CM, Shiffer KA, Mortimore GE. Quantitative relationship between autophagy and proteolysis during graded amino acid deprivation in perfused rat liver. *J Biol Chem* 1981;256:7652–7658.
15. Blommaert EFC, Luiken JJ, Blommaert PJ, et al. Phosphorylation of ribosomal protein S6 is inhibitory for autophagy in isolated rat hepatocytes. *J Biol Chem* 1995;270:2320–2326.
16. Patti ME, Brambilla E, Luzi L, et al. Bidirectional modulation of insulin action by amino acids. *J Clin Invest* 1998;101:1519–1529.
17. Hara K, Yonezawa K, Weng QP, et al. Amino acid sufficiency and mTOR regulate p70 S6 kinase and eIF-4E BP1 through a common effector mechanism. *J Biol Chem* 1998;273:14484–14494.
18. Mordier S, Deval C, Béchet D, et al. Leucine limitation induces autophagy and activation of lysosome-dependent proteolysis in C₂C₁₂ myotubes through a mammalian target of rapamycin-independent signaling pathway. *J Biol Chem* 2000;275:29900–29906.
19. Kanazawa T, Taneike I, Akaishi R, et al. Amino acids and insulin control autophagic proteolysis through different signaling pathways in relation to mTOR in isolated hepatocytes. *J Biol Chem* 2004;279:8452–8459.
20. Kadowaki M, Karim MR, Carpi A, et al. Nutrient control of macroautophagy in mammalian cells. *Mol Aspects Med* 2006;27:426–443.
21. Moore MN, Allen JJ, Somerfield PJ. Autophagy: role in surviving environmental stress. *Mar Environ Res* 2006;62:S420–S425.
22. Sartor RB. Induction of mucosal immune responses by bacteria and bacterial components. *Curr Opin Gastroenterol* 2001;17:555–561.
23. Ko TC, Beauchamp RD, Townsend CM Jr, et al. Glutamine is essential for epidermal growth factor-stimulated intestinal cell proliferation. *Surgery* 1993;114:147–153.
24. Scheppach W, Loges C, Bartram P, et al. Effect of free glutamine and alanyl-glutamine dipeptide on mucosal proliferation of the human ileum and colon. *Gastroenterology* 1994;107:429–434.
25. Buchman AL, Moukarzel AA, Bhuta S, et al. Parenteral nutrition is associated with intestinal morphologic and functional changes in humans. *JPN J Parenter Enteral Nutr* 1995;19:453–460.
26. Van der Hulst RR, van Kreel BK, von Meyenfeldt MF, et al. Glutamine and the preservation of gut integrity. *Lancet* 1993;341:1363–1365.
27. Musch MW, Ciancio MJ, Sarge K, et al. Induction of heat shock protein 70 protects intestinal epithelial IEC-18 cells from oxidant and thermal injury. *Am J Physiol* 1996;270:C429–C436.
28. Wischmeyer PE, Musch MW, Madonna MB, et al. Glutamine protects intestinal epithelial cells: role of inducible HSP70. *Am J Physiol* 1997;272:G879–G884.
29. Wischmeyer PE, Riehm J, Singleton KD, et al. Glutamine attenuates tumor necrosis factor- α release and enhances heat shock protein 72 in human peripheral blood mononuclear cells. *Nutrition* 2003;19:1–6.
30. Coëffier M, Marion R, Ducrotté P, et al. Modulating effect of glutamine on IL-1 β -induced cytokine production by human gut. *Clin Nutr* 2003;22:407–413.
31. Singleton KD, Beckey VE, Wischmeyer PE. Glutamine prevents activation of NF- κ B and stress kinase pathways, attenuates inflammatory cytokine release, and prevents acute respiratory distress syndrome (ARDS) following sepsis. *Shock* 2005;24:583–589.
32. Harward TR, Coe D, Souba WW, et al. Glutamine preserves gut glutathione levels during intestinal ischemia/reperfusion. *J Surg Res* 1994;56:351–355.
33. Evans ME, Jones DP, Ziegler TR. Glutamine inhibits cytokine-induced apoptosis in human colonic epithelial cells via the pyrimidine pathway. *Am J Physiol Gastrointest Liver Physiol* 2005;289:G388–G396.
34. Paquette JC, Guérin PJ, Gauthier ER. Rapid induction of the intrinsic apoptotic pathway by L-glutamine starvation. *J Cell Physiol* 2005;202:912–921.
35. Fuchs BC, Bode BP. Stressing out over survival: glutamine as an apoptotic modulator. *J Surg Res* 2006;131:26–40.
36. Onodera J, Ohsumi Y. Autophagy is required for maintenance of amino acid levels and protein synthesis under nitrogen starvation. *J Biol Chem* 2005;280:31582–31586.
37. Kuma A, Hatano M, Matsui M, et al. The role of autophagy during the early neonatal starvation period. *Nature* 2004;432:1032–1036.
38. Periyasamy-Thandavan S, Jiang M, Wei Q, et al. Autophagy is cytoprotective during cisplatin injury of renal proximal tubular cells. *Kidney Int* 2008;74:631–640.
39. Ogawa M, Yoshimori T, Suzuki T, et al. Escape of intracellular *Shigella* from autophagy. *Science* 2005;307:727–731.
40. Gutierrez MG, Saka HA, Chinen I, et al. Protective role of autophagy against *Vibrio cholerae* cytolysin, a pore-forming toxin from *V. cholerae*. *Proc Natl Acad Sci U S A* 2007;104:1829–1834.
41. Hampe J, Franke A, Rosenstiel P, et al. A genome-wide association scan of nonsynonymous SNPs identifies a susceptibility variant for Crohn disease in ATG16L1. *Nat Genet* 2007;39:207–211.
42. Rioux JD, Xavier RJ, Taylor KD, et al. Genome-wide association study identifies new susceptibility loci for Crohn disease and implicates autophagy in disease pathogenesis. *Nat Genet* 2007;39:596–604.
43. Parkes M, Barrett JC, Prescott NJ, et al. Sequence variants in the autophagy gene IRGM and multiple other replicating loci contribute to Crohn's disease susceptibility. *Nat Genet* 2007;39:830–832.
44. Singh SB, Davis AS, Taylor GA, et al. Human IRGM induces autophagy to eliminate intracellular mycobacteria. *Science* 2006;313:1438–1441.
45. Codogno P, Meijer AJ. Autophagy and signaling: their role in cell survival and cell death. *Cell Death Differ* 2005;12(Suppl 2):1509–1518.
46. Krause U, Bertrand L, Maisin L, et al. Signalling pathways and combinatory effects of insulin and amino acids in isolated rat hepatocytes. *Eur J Biochem* 2002;269:3742–3750.
47. Nakajo T, Yamatsuji T, Ban H, et al. Glutamine is a key regulator for amino acid-controlled cell growth through the mTOR signaling pathway in rat intestinal epithelial cells. *Biochem Biophys Res Commun* 2005;326:174–180.
48. Deldicque L, Sanchez Canedo C, Horman S, et al. Antagonistic effects of leucine and glutamine on the mTOR pathway in myogenic C₂C₁₂ cells. *Amino Acids* 2008;35:147–155.
49. Häussinger D, Schliess F, Dombrowski F, et al. Involvement of p38MAPK in the regulation of proteolysis by liver cell hydration. *Gastroenterology* 1999;116:921–935.
50. Comes F, Matrone A, Lastella P, et al. A novel cell type-specific role of p38 α in the control of autophagy and cell death in colorectal cancer cells. *Cell Death Differ* 2007;14:693–702.

Received June 10, 2008. Accepted December 1, 2008.

Reprint requests

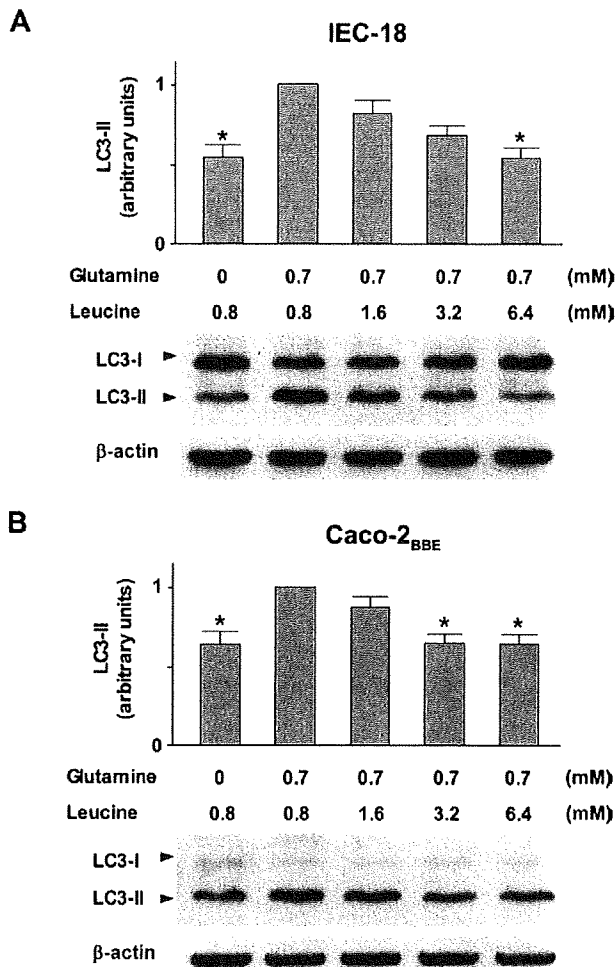
Address requests for reprints to: Eugene B. Chang, MD, Martin Boyer Laboratories, University of Chicago IBD Research Center, 5841 S. Maryland Avenue, MC6084, Chicago, Illinois 60637. e-mail: echang@medicine.bsd.uchicago.edu; fax: (773) 702-2281.

Conflict of interest

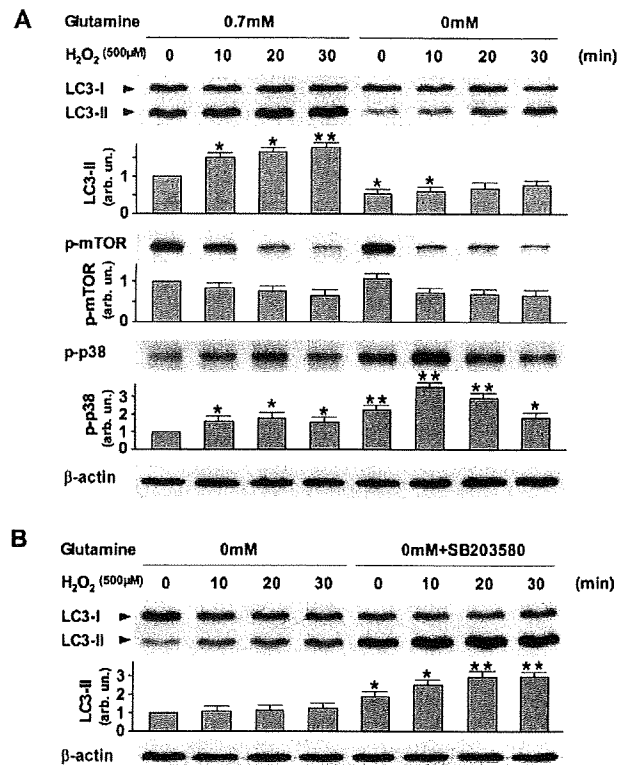
The authors disclose no conflicts.

Funding

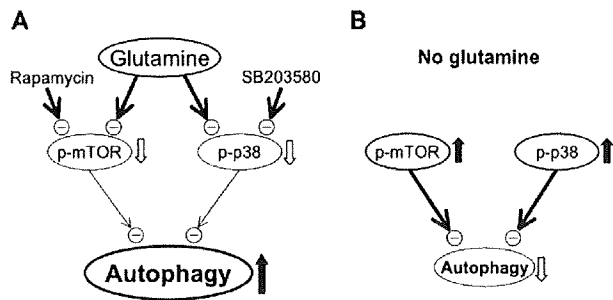
This work was supported by National Institutes of Health grants DK-47722, DK-38510 (to E.B.C.), and the Digestive Disease Research Core Center grant DK-42086, a grant from the Crohn's and Colitis Foundation of America, and the Gastrointestinal Research Foundation of Chicago.



Supplementary Figure 1. Leucine antagonizes glutamine's enhancement of autophagy in IEC-18 and Caco-2_{BBE} cells. (A) IEC-18 cells were incubated with 0 mmol/L glutamine or 0.7 mmol/L glutamine and designated concentrations of leucine for 24 hours, and analyzed by Western blotting. (B) Caco-2_{BBE} cells were incubated with 0 mmol/L glutamine or 0.7 mmol/L glutamine and designated concentrations of leucine for 24 hours, and analyzed by Western blotting. The ratio of LC3-II to β-actin density was calculated using ImageJ software, and set to 1 for 0.7 mmol/L glutamine and 0.8 mmol/L leucine. Images are representative of 3 separate experiments. Data are shown as means ± SE. **P* < .05 compared with 0.7 mmol/L glutamine and 0.8 mmol/L leucine by ANOVA using a Bonferroni correction.



Supplementary Figure 2. Glutamine depletion decreases the autophagy response to oxidative stress by the activation of p38 MAP kinase. (A) Decreased autophagy response to H₂O₂-induced oxidative stress in glutamine-depleted cells. IEC-18 cells were incubated with 0.7 mmol/L glutamine (4 left lanes) or without glutamine (4 right lanes) for 24 hours. Cells subsequently were treated with 500 μmol/L H₂O₂, collected at designated times and analyzed by Western blotting. Images are representative of 3 separate experiments. Densitometric values were obtained using ImageJ software and normalized to β-actin, set to 1 for unstimulated conditions in 0.7 mmol/L glutamine. Data are shown as means ± SE. **P* < .05 and ***P* < .01 compared with unstimulated conditions and 0.7 mmol/L glutamine by ANOVA using a Bonferroni correction. (B) Inhibition of p38 MAP kinase restores the normal autophagy response to H₂O₂-induced oxidative stress in glutamine-depleted cells. IEC-18 cells were incubated in glutamine-depleted media without SB203580 (4 left lanes) or with 5 μmol/L SB203580 (4 right lanes) for 24 hours. Cells subsequently were treated with 500 μmol/L H₂O₂, collected at designated times and analyzed by Western blotting. Images are representative of 3 separate experiments. The ratio of LC3-II to β-actin density was calculated using ImageJ software, and set to 1 for unstimulated conditions without glutamine and SB203580. Data are shown as means ± SE. **P* < .05 and ***P* < .01 compared with unstimulated conditions, 0 mmol/L glutamine, and no SB203580 by ANOVA using a Bonferroni correction.



Supplementary Figure 3. Model of glutamine regulation of autophagy. (A) Glutamine inhibits the activity of mTOR and p38 MAP kinase, which are negative regulators of autophagy. Hence, the presence of glutamine inhibits 2 inhibitory pathways of autophagy, resulting in increased autophagy. Inhibition of mTOR and p38 MAP kinase (ie, rapamycin and SB203580) mimics glutamine's effect by suppressing these negative regulators of autophagy. (B) In the absence of glutamine, mTOR and p38 MAP kinase are activated, thereby suppressing autophagy.